Sulfate and acid resistance of lithomarge-based geopolymer mortars

Kwasny, J., Aiken, T. A., Soutsos, M. N., McIntosh, J. A., & Cleland, D. J. (2018). Sulfate and acid resistance of lithomarge-based geopolymer mortars. *Construction and Building Materials*, *166*, 537-553. https://doi.org/10.1016/j.conbuildmat.2018.01.129

Published in:
Construction and Building Materials

Document Version:
Peer reviewed version

Sulfate and acid resistance of lithomarge-based geopolymer mortars

Jacek Kwasny[a,1*], Timothy Aiken[a,2], Marios N. Soutsos[a,3], John A. McIntosh[a,b,4], and David J. Cleland[a,5]

[a] School of Natural and Built Environment, Queen's University Belfast,

Belfast BT9 5AG, UK

[b] banah UK Ltd, 1b Letterloan Road, Macosquin, Northern Ireland, BT51 4PP

[1] j.kwasny@qub.ac.uk (* corresponding author)

[2] taiken02@qub.ac.uk

[3] m.soutsos@qub.ac.uk

[4] andrew@banahuk.co.uk

[5] d.cleland@qub.ac.uk

ABSTRACT

The resistance of room temperature cured geopolymer mortars (GPM) against chemical attacks, i.e. sodium and magnesium sulfate solutions, and sulfuric and hydrochloric acid solutions, was evaluated. GPMs were formulated using a lithomarge precursor (low-purity kaolin) to achieve 28-day characteristic compressive strengths of 37.5 and 60 MPa. Their performance was compared with those of equivalent Portland cement mortars (PCMs) having the same paste volume and strength grade. GPMs with both strength grades showed superior performance against sulfate attack when compared to PCMs. No visual deterioration was observed in GPMs, the mass and length changes were relatively small, and no changes to the microstructure were detected – in contrast to severely deteriorated PCMs.

As confirmed by visual observations and lower mass loss, GPMs showed better resistance to attack by both acids than PCMs. GPMs provided a better quality (lower permeability) of an acid-degraded layer, lowering the degree of further deterioration. The main mechanisms of the matrix deterioration of GPMs in both acids was dealumination of the hardened binder, with a higher degree of changes detected for sulfuric acid.

Keywords: Lithomarge; Geopolymer mortars; Portland cement mortars; Durability; Sulfate attack; Sodium sulfate; Magnesium sulfate; Acid attack; Sulfuric acid; Hydrochloric acid;

1 INTRODUCTION

Portland cement based concrete, being the most versatile and widely used construction material, frequently operates in environments where it is exposed to aggressive aqueous media. Contact of highly alkaline (pH > 12.5) hardened cement paste (hcp) with water carrying aggressive ions can cause chemical as well as physical degradation [1, 2]. Three common types of chemical degradation mechanisms are: an ion exchange reaction between aggressive medium and the hardened binder, reaction leading to leaching of ions from the hcp, and reaction causing growth of expansive products within the pore structure of hcp [1]. These chemical processes often occur simultaneously and are directly responsible for physical changes to the hcp microstructure, i.e. altering porosity, permeability and integrity of the concrete [2]. With respect to the aggressive species, two common types of chemical attack are external sulfate attack and acid attack [3-6].

External sulfate attack is associated with applications where a structural element is in contact with sulfate-rich environments such as contaminated soil or ground water, sea water or wastewater treatment infrastructure [4, 5]. Severity and extent of the attack depends on

factors related to concrete itself, such as the type of cement used and the overall quality of concrete, but also on the properties of the aggressive medium, e.g. sulfate ion concentration and mobility, type of the cation (most common being Na^+, K^+, Mg^{2+} and Ca^{2+}), or pH. [4, 5]. In the majority of sulfate attacks, the most vulnerable compounds to react with waterborne sulfate ions are calcium hydroxide (CH) and phases containing aluminium, such as AFm (*e.g.* monosulfate) and unreacted C_3A [5-7]. Reactions will result in the formation of expansive salt crystals, such as ettringite and gypsum (with ettringite being more devastating than gypsum [8]), within the hcp pore structure [9]. Consequently, expansion and cracking result in severely compromised structural integrity of the attacked concrete. Cracking also leads to further propagation of the attack.

Concrete can be exposed to a wide range of attacks caused by both organic and inorganic acids [5, 10]. Acidic media can originate from agriculture, urban and industrial human activities, as well as occurring naturally [5, 10]. The severity of acid attack, in addition to composition and quality of the concrete, depends on: the acid type; concentration and pH of the acid solution; on the availability of acid solution to react with concrete; and finally – on the medium surrounding the concrete (whether it flows and/or contains abrasive particles) [11, 12]. The focus of this work is on strong mineral acids, namely sulfuric acid (H_2SO_4) and hydrochloric acid (HCl). Their actions lead to strong decalcification of the hcp, and then (at lower pH) to removal of Al^{3+} and Fe^{3+} [5, 10]. The order of dissolution of calcium bearing phases is as follows: CH > AFm > AFt > C-S-H [12, 5]. In the course of decalcification new compounds are precipitated and, depending on their solubility in water, they may leach out or remain in the pore structure [12]. The action of H_2SO_4 is especially severe because the acid attack is coupled with the sulfate attack [5]. Progression of the acid attack front causes loss of alkalinity coupled with an increase in porosity and permeability, thus leading to mass and strength loss [12]. Inability to maintain Ca^{2+} ion concentration in

the hcp and a more open microstructure of the altered zone causes further ingress of the attack front [12].

As a result of the typically low resistance of Portland cement based materials to the actions of sulfate and acid attack, the service life of the exposed structure is reduced. This has multifaceted consequences: financial, social and environmental, associated with costly maintenance or replacement of the damaged structure. The problem of chemical attack may be addressed by applying layers of sealants or coatings on the concrete surface, or creating a physical barrier between concrete and the aggressive environment via protective overlays [13-15]. This should limit/prevent ingress of aggressive media into the concrete microstructure. Whilst effective, these solutions proved to be costly and labour intensive [16]. An alternative approach is to improve the performance of concrete by modifying its composition; however, such solutions vary in effectiveness. Typically, to improve sulfate resistance of concrete, either cements with reduced C_3A content are used (sulfate resistant cements) or reduced CH content and permeability of hcp are sought after, for instance by using blended cements [5, 17-19]. The resistance of cement-based materials to acid attack strongly depends on the content and type of calcium bearing hydration products [11], intrinsic permeability of undamaged concrete [11] and most importantly – on the permeability of the acid-degraded layer [12]. To improve these features, investigations were conducted into the use of blended cements, partial replacement of Portland cement with additions (also called supplementary cementitious materials) or use of polymer modified cements. However, conflicting reports on their effectiveness to provide acid resistance are reported [20-26]. Recently, a promising solution has emerged in the form of geopolymer binders which have been reported to have improved resistance to sulfate [27-33] and acid attack [21, 27, 30, 31, 34-39] due to their ceramic-like microstructure.

Geopolymers are a low-carbon alternative to Portland cement-based binders in mortar and concrete. They typically consist of a powder precursor, primarily composed of amorphous alumino-silicates, and a liquid chemical activator containing an alkali source, providing elevated pH, in the form of hydroxides, silicates, or their blends [40]. When mixed, the two components undergo a dissolution/condensation reaction to form a ceramic-like amorphous microstructure [40]. Geopolymers are a sub-group of a much wider group of materials, called alkali activated materials [41].

As the definition currently stands [40, 42], there is a wide range of potential precursors and activators that may be used and which would produce geopolymers of varying quality. In terms of the precursor, the most common candidates are high purity kaolin [43, 44] and different types of clays [45-47], or waste/by-product materials, such as slags [40] and ashes [40, 48-50]. However, some of these materials may not be readily available across the globe or are too expensive. It is well known that in the UK and Europe, the supply of good quality fly ash for concrete applications is limited [51] and will become more so due to the move away from fossil fuels for electricity generation [52]. While almost all of the UK produced slag is used in cement production, a continuous demand of fly ash for use in blended cements or as partial replacement of Portland cement will cause increased pressure on its supplies [51]. Heath *et al.* [53] anticipated that current global production of fly ash and slag cement meets only 20% of PC demand and will most likely fall below 10% by 2050. It is estimated that, despite being limited, the UK has larger resources of kaolin than fly ash [51]. However, high costs involved in the production of high purity metakaolin (made from clays containing at least 85% kaolin [54]), render it uneconomical for use in the majority of geopolymer concrete and mortar applications [55]. Consequently, locally available clays with lower kaolin content are of interest. Some of them have already been reported to produce geopolymer binders with compressive strength of at least 50 MPa upon calcination

[56-61]. In Northern Ireland, a large deposit of metamorphose lateritic lithomarge forms a part of the Interbasaltic Formation (IBF) [62]. Lithomarge is a soft rock, primarily containing kaolinite ($Al_2Si_2O_5(OH)_4$), gibbsite ($Al(OH)_3$), goethite ($FeO(OH)$), hematite (Fe_2O_3) and various smectite minerals [63]. Geopolymer binders with strength exceeding 50 MPa were successfully formulated with calcined lithomarge obtained from rocks containing at least 60% w/w of kaolinite [60].

Sulfate and acid attack on clay based geopolymer binder systems has previously been investigated using geopolymers formulated with pure metakaolin [27, 33, 36, 38, 39]. In order to encourage the use of less expensive kaolin geopolymer binders, this research aimed to assess and directly compare the resistance of lithomarge-based geopolymer and neat Portland cement mortars to chemical attack by sulfate (Na_2SO_4 and $MgSO_4$) and mineral acid (H_2SO_4 and HCl) solutions. Mortars were formulated with characteristic compressive strengths of 37.5 and 60 MPa, to additionally assess the influence of strength grades on the resistance to chemical attack.

2 EXPERIMENTAL PROGRAMME

The methodology of the research will be outlined, followed by the description of materials and mix proportions used. Mortar mixing and sample preparation will then be described, followed by the presentation of testing procedures.

2.1 Methodology

To allow for a like-for-like comparison, two geopolymer mortar (GPM) mixes and two Portland cement mortar (PCM) mixes were selected from work reported elsewhere [61]. Mortars with both binders were optimised to have equivalent paste volumes of 500 L/m^3 and

characteristic 28-day compressive strengths to satisfy normal (37.5 MPa) and high strength concrete (>60 MPa) applications.

In order to determine resistance of mixes to sulfate attack, 28-day old bar samples were stored in 0.352 mol/L solutions of sodium sulfate (Na_2SO_4) or magnesium sulfate ($MgSO_4$) for a total duration of 52 weeks. To assess the degree of sulfate attack, the following properties were tested periodically: visual appearance, mass change and length change. In addition, pH of sulfate solutions used for storing the samples was measured. Microstructural changes were determined after 56 weeks of testing by X-ray diffraction (XRD) and FTIR spectroscopy, on sulfate exposed and control (stored in water) samples of the high strength GPM and PCM mixes.

Resistance to acid attack was determined by immersing 28-day old cube samples in either H_2SO_4 or HCl solutions for 8 weeks. Three concentrations of each acid solution were used, *i.e.* 0.10, 0.31 and 0.52 mol/L. Samples were tested weekly for visual appearance and mass change. The pH of acid solutions was measured on regular intervals throughout the week, and the solution was replenished on weekly basis. Microstructural changes were evaluated by comparing the high strength samples exposed to 0.52 mol/L acid solutions with control samples stored in water, using both XRD and FTIR spectroscopy.

2.2 Materials

The geopolymer binder was a two-part system produced by banah UK Ltd [64]. It comprised a powder component, based on a calcined kaolinite-rich clay (here called calcined lithomarge), and a liquid component, *i.e.* chemical activator – see Figure 1. The ferruginous kaolinitic clay, which was an altered basalt (lithomarge), was sourced from the IBF of the Antrim Lava Group (Northern Ireland) [59-61]. It was calcined at 750 °C to achieve dehydroxylation of the clay minerals and milled to a particle size distribution with d_{90} passing

a 56 μm sieve. Portland cement CEM I 42.5N produced in Northern Ireland and conforming to the requirements of BS EN 197-1:2011 [65] was used. Chemical compositions (determined using X-ray fluorescence spectrometry), crystal structure (determined with X-ray powder diffraction spectrometry) and particle size distribution of calcined lithomarge and Portland cement are given in Table 1, Figure 2 and Figure 3, respectively. The main peaks in the XRD pattern of calcined lithomarge are due to hematite (H), which is present as a result of calcination of goethite and magnetite in the original kaolinite clay [59]. Crystalline phases including alite (AE), belite (BE), aluminate (AL), brownmillerite (BR) and gypsum (G) are present in Portland cement.

Figure 1: Liquid activator and powder component produced by banah UK Ltd.

Table 1: Oxide composition and physical properties of calcined lithomarge and Portland cement.

Oxide composition [%]	Calcined lithomarge	Portland cement
SiO_2	32.04	20.21
Al_2O_3	24.99	4.79
Fe_2O_3	25.21	2.78
CaO	7.78	63.01
MgO	1.71	1.93
MnO	0.37	0.08
TiO_2	3.17	0.27
Na_2O	0.36	0.19
K_2O	0.15	0.59
SO_3	0.22	2.60
P_2O_5	0.14	0.12
LOI [%]	3.08	3.16
Specific gravity	2.89	3.13

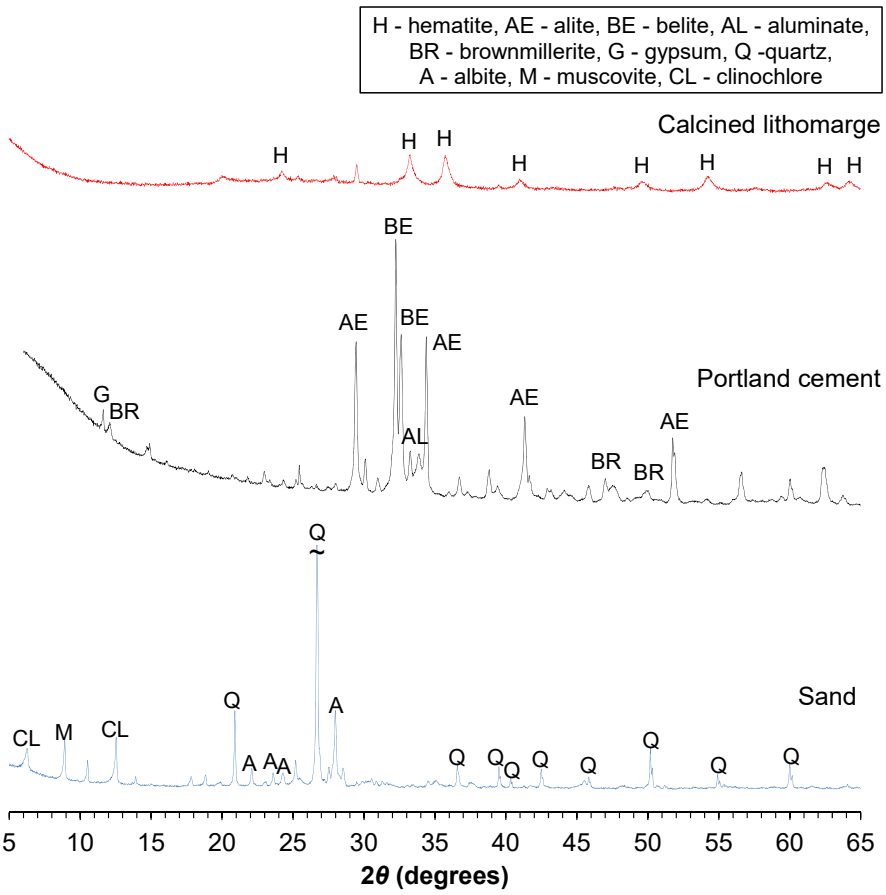

Figure 2: XRD patterns of calcined lithomarge, Portland cement and sand.

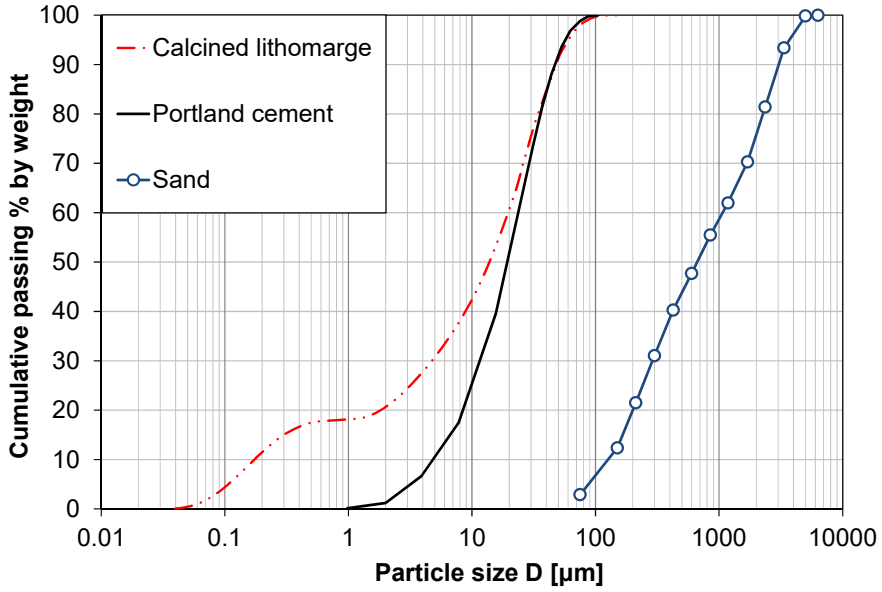

Figure 3: Particle size distribution of calcined lithomarge, Portland cement and sand.

A proprietary chemical activator was an aqueous solution of alkali silicate with a water content of 41.2% and specific gravity of 1.57. Water from the mains supply (17 ±1 °C) was used as the mixing water.

Sand, with oven-dry particle density of 2695 kg/m^3 was sourced from Creagh's quarry (Creagh Concrete Products Ltd., Draperstown, Northern Ireland). Water absorption of sand at 1-hour and 24-hours was 0.92% and 1.1%, respectively. Both density and water absorption were determined according to BS 812-2:1995 [66]. The aggregate particle size distribution was determined according to BS 812-103.1:1985 [67] and is shown in Figure 3. As demonstrated in Figure 2, sand was abundant in quartz (Q) and also contained albite (A), muscovite (M) and clinochlore (CL).

Laboratory reagent grade chemicals, *i.e.* anhydrous sodium sulfate (Na_2SO_4), anhydrous magnesium sulfate ($MgSO_4$), concentrated sulfuric acid (95-97% H_2SO_4) and hydrochloric acid (≥37% HCl), were used to prepare testing sulfate and acid solutions by mixing in various proportions with distilled water.

2.3 Mortar proportions

The proportions of all mortars are shown in Table 2. They were selected from the range of mixes previously reported by Kwasny *et al.* [61]. Mortars were designed following the recommendation of the absolute volume method [68].

Table 2: Mix proportions of GPM and PCM mixes.

Mix ID	w/s ratio	w/c ratio	Paste volume [L/m^3]	Material quantity per cubic metre [kg/m^3]						
				Calcined lithomarge	Chemical activator	Portland cement	Sand	Absorption water	Total added water	Free water
GPM-37.5	0.375	-	500	482	342	-	1347	12.4	128	256
GPM-60	0.275	-	500	559	396	-	1347	12.4	67	218
PCM-37.5	-	0.600	500	-	-	544	1347	12.4	339	326
PCM-60	-	0.420	500	-	-	676	1347	12.4	296	284

2.4 Mix preparation

Sand, after oven drying for at least 48 hours at 105 ±5 °C, was stored in plastic bags until mixing. All constituent materials were stored in dry locations at room temperature (20 ±2 °C) prior to batching, to ensure that no other parameters influenced the results.

Mortars were prepared in a 10 L capacity planar-action high-shear mixer, in 6 L batches. The mixing procedure consisted of six steps. Sand was placed in a mixer's pan with half of the total water (free + absorption water) and mixed for approximately 1 minute (Step 1). Step 1 was initiated approximately 15 minutes before Step 2. The dry portion of binding material, *i.e.* calcined lithomarge or Portland cement, was introduced into the mixing bowl followed by 1 minute of mixing at low speed (Step 2). The remaining half of the total water and, in the case of GPMs, the chemical activator, were added to the mixing bowl and mixed for 2 minutes at low speed (Step 3). The mixer was stopped for 1 minute to crush any lumps of remaining solids (Step 4). Afterwards, mixing resumed for 2 minutes at a high speed (Step 5), followed by 1 minute at a low speed (Step 6).

2.5 Sample casting, demoulding and conditioning

The following mortar samples were cast for each mix: twenty six 50×50×50 mm cubes and six 25×25×285 mm bars. Samples were cast in two layers, with each layer compacted on a vibrating table. Afterwards, they were wrapped with cling film to prevent water evaporation and placed in the conditioning room (RH >95% and 20 ±1 °C). Samples were demoulded at 24 ±0.5 hours, counting from the beginning of step 3 of the mixing procedure, and placed in curing containers on 15 mm height spacers. The curing containers were filled with water to the height of 5 mm, then covered with tightly fitting lids and stored in the conditioning room (20 ±1 °C). This procedure allowed the conditioning of the samples

at RH of >95% and prevented unintentional carbonation of the samples, and leaching of alkalis. After 21 days of curing, the samples were transferred to a water bath (20 ±1 °C) until 28-day, in order to ensure full water saturation before starting sulfate and acid testing. At 28-day, two control (unexposed) cube samples were left in the water bath for further testing. Separate water baths were used for each mix in order to avoid cross contamination due to leaching.

2.6 Testing procedures

Resistance to sulfate attack was tested in similar way to the procedure described in ASTM C1012 [69] by measuring the length change of mortar samples immersed in sulfate solutions. The samples were 25×25×285 mm mortar bars equipped with 6 mm diameter stainless steel balls at each end. The length of the bars was measured initially at 28-day after casting, and then sets of three bars from each mix were placed vertically in airtight plastic storage containers filled with 0.352 moles of Na_2SO_4 or $MgSO_4$ per litre of solutions (equivalent to 5% and 4.24% concentrations, respectively). The proportion of sulfate solution volume to samples volume in a storage container was kept at approximately 4.4 (*i.e.* 800 mL of solution per mortar bar). Samples were kept in the sulfate solutions (20 ±1 °C) for a total of 52 weeks, during which their length and mass were measured at specific intervals (every week for the duration of the first 4 weeks, then every two weeks for the duration of 8 weeks, and 4 weeks for the remaining 40 weeks). At the same time, the pH of the sulfate solutions was also measured. Before the length and mass measurements were determined, samples were visually inspected and their surface was gently dried by hand with a moist paper towel to achieve saturated and surface-dry condition. During the first 12 weeks of testing, sulfate solutions were renewed every 2 weeks, and every 4 weeks afterwards. The length change, expressed in microstrain, was calculated for the nominal gauge length of

280 mm (innermost distance between stainless steel balls) and is reported as an average of three measurements. In addition, the relative mass change of bars, given in % of the 28-day mass, was calculated and the average is reported. After 52 weeks of testing, samples were collected from the outermost surface layer of the mortar bars exposed to sulfate solution (no deeper than 0.5 mm) and from the middle of the fractured control cube sample kept in water bath. These samples were transferred to airtight bottles and then further processed, as indicated below, for XRD and FTIR spectroscopy analysis.

Resistance to inorganic H_2SO_4 and HCl acid attack was determined using an accelerated method, based on the general guidelines provided in ASTM C267 [70]. Mass loss of mortar samples, *i.e.* 50 mm size cubes, immersed in acid solution, was investigated. At 28-day the mass of each cube was measured and sets of four cubes from each mix were placed in plastic boxes containing acid solutions (20 ±1 °C) with concentrations of 0.10, 0.31 and 0.52 moles of H_2SO_4 (*i.e.* 1%, 3% and 5%) or HCl (*i.e.* 0.37%, 1.12% and 1.86%) per litre of solution. The volume proportion of acid solution to samples in a storage container was approximately 0.9. Every 7 days, any loose material was removed from each sample by gentle brushing under a stream of tap water. Then, surface of each sample was gently dried by hand with a moist paper towel to achieve saturated and surface-dry condition. Visual inspection was subsequently carried out and the mass of each cube was recorded. Before disposing, the used acid solutions were filtered to collect the debris material remaining in the storage boxes. Cube samples were returned to the boxes, filled with fresh acid solutions. This procedure was repeated for 8 consecutive weeks. An average cumulative mass loss is reported. In addition, pH of the acid solution was recorded at suitable intervals, *i.e.* at 1, 5 and 7-day after the acid solution was replenished. Collected debris material from storage boxes, and that from the middle of the fractured control cube sample kept in water bath, were placed in airtight bottles for further processing prior to XRD and FTIR examination.

After collection, samples for XRD and FTIR spectroscopy studies were transferred to a desiccator and stored for *ca.* 24 hours under vacuum at 40 ±1 °C to evaporate the moisture. Then, dried samples were powdered using mortar and pestle to pass a 63 μm sieve. Immediately after grinding, the powdered samples were placed in sealable plastic bags and stored in the desiccator under vacuum at 20 ±1 °C until testing.

Powdered samples were analyzed using XRD, with a PANalytical X'Pert PRO diffractometer, to identify the crystalline components and observe potential changes caused by either sulfate or acid attack. Diffraction patterns were collected between 5° and 65° 2θ with a step size of 0.016°. PANalytical X'Pert Highscore software with the Powder Diffraction File database was used to identify the mineralogy of the samples based on the diffraction patterns.

To qualitatively identify bond degradation due to sulfate and acid attack, powdered samples were analyzed using FTIR spectroscopy. A Jasco 4100 series FTIR Spectrometer with Attenuated Total Reflectance attachment (germanium crystal) was used. The spectra were recorded between 650 and 4000 cm^{-1}.

Mercury intrusion porosimetry (MIP) was used to assess the pore structure of mortars. At 28 days mortar fragments measuring approximately 8×8×20 mm, were extracted from the core of each cube. Hydration/reaction was stopped by oven drying the samples for 24 hours in 60 ±1 °C and then immersing them in acetone for 4 hours and subsequent drying in a desiccator (20 ±1 °C) for further 24 hours. The pore structure of the samples was then determined using a Pascal 140/240 mercury intrusion porosimeter from Thermo Scientific. The mercury contact angle was taken to be 140°.

3 RESULTS AND DISCUSSION

The porosity and the pore structure of geopolymer and Portland cement based mortars are first compared, as they are expected to affect the resistance to chemical attack. The effect of sulfate and acid attacks on physical and microstructural features of these mortars are then discussed.

3.1 Pore structure and porosity

The pore size distribution and the pore structure properties of mortar samples are shown in Figure 4 and summarised in Table 3. It is worth noting that, due to MIP test limitations, its use to characterise the pore size distribution of cementitious materials has been criticised [71]. However, here the MIP was used mainly to compare between the tested materials.

It can be seen that for GPMs most of the pores have diameter below 0.050 μm while for PCMs they were between 0.020 and 0.200 μm (Figure 4). It is clear that geopolymer mixes had lower threshold pore diameter and porosity, and higher total pore surface area than their cement counterparts (Table 3). This is similar to findings reported elsewhere [33].

When strength grade is compared for mixes made with the same binder type, mixes with higher compressive strength (lower w/s ratio for GPMs or w/c ratio for PCMs) showed lower threshold pore diameter, porosity and total surface area of pores. Therefore, in this respect, GPMs were similar to typical Portland cement systems, where porosity and size of pores are mainly controlled by w/c ratio. These trends are in good agreement with data found in the literature for both geopolymers formulated with metakaolin [33, 72, 73] and Portland cement systems [74, 75].

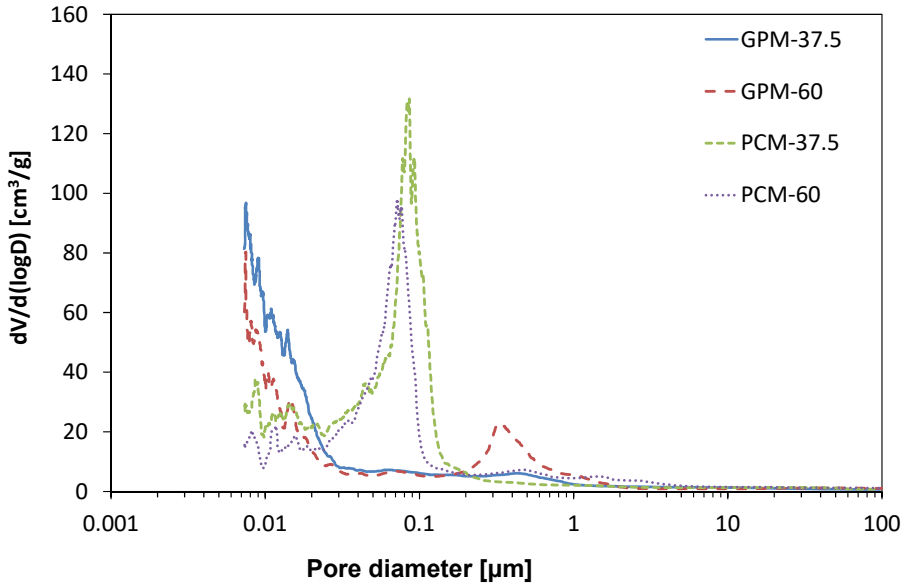

Figure 4: Differential volume of intruded mercury versus pore diameter for mortar at the age of 28 days.

Table 3: Pore structure properties of mortars at the age of 28 days.

Binder type	Geopolymer-based		PC-based	
Characteristic strength class	37.5 MPa	60 MPa	37.5 MPa	60 MPa
Mix ID	GPM-37.5	GPM-60	PCM-37.5	PCM-60
Threshold pore diameter [µm]	0.027	0.025	0.155	0.115
Porosity [%]	8.6	7.3	12.0	10.1
Total surface area [m^2/g]	9.99	6.55	6.64	4.51

3.2 Resistance to sulfate attack

The resistance of PCM and GPM samples to sulfate attack is presented in this section. Description of the changes in visual appearance of samples immersed in Na_2SO_4 and $MgSO_4$ solutions is followed by changes in the pH of sulfate solutions, mass changes of samples, length changes of samples, microstructural changes of samples determined by XRD analysis and FTIR spectroscopy, and finally a summary of the findings is presented.

3.2.1. Visual appearance

The visual appearance of samples after 52 weeks of exposure to solutions of 0.352 mol/L of Na_2SO_4 and $MgSO_4$ are shown in Figure 5. There was no sign of discoloration,

expansion or cracking on the surface of any of the GPM samples. In contrast, PCM samples showed variable degree of deterioration. Surfaces of PCM samples stored in Na_2SO_4 solutions were covered with a net of microcracks (Figure 5a). The samples were curled, broken, and longitudal and lateral expansion was easily noticeable. Surfaces of PCM samples exposed to $MgSO_4$ solution were coated with a layer of white precipitates (Figure 5b), which has been confirmed as magnesium sulfate hydrate (section on XRD). Edges of PCM samples became rounded, due to loss of degraded material. Although PCM samples showed visible expansion, they maintained their initial shape.

In general, no effect of strength grade was detected for geopolymer mixes, while for PCMs the normal strength mixes showed higher deterioration in both solutions. The PCM-37.5 samples exposed to Na_2SO_4 fragmented, due to expansion, expansive spalling and cracking, after week 24 of the test and their colour changed to light grey (PCM-37.5 sample shown in Figure 5a was carefully reassembled to illustrate the degree of deterioration and expansion). The visual degradation of PCMs is in good agreement with the literature [76, 77].

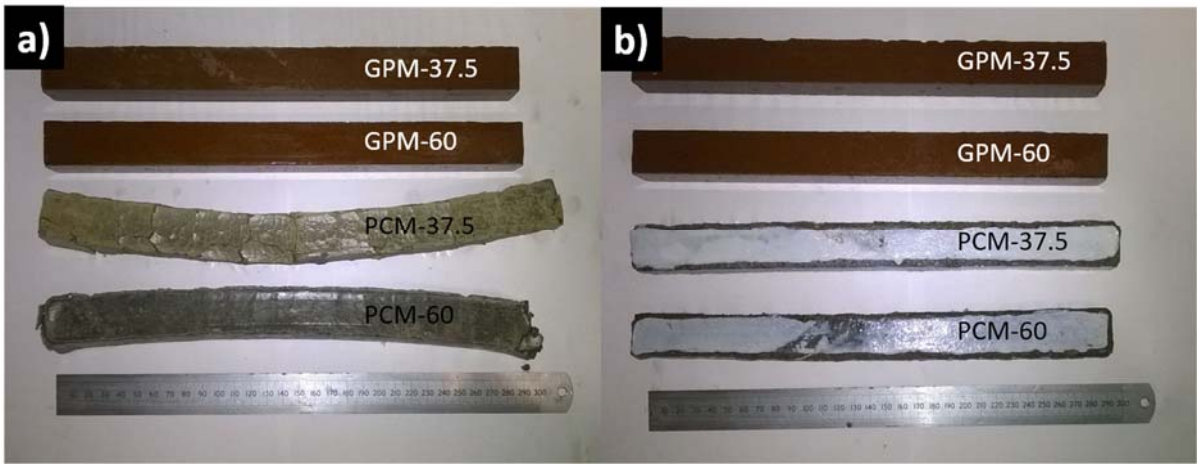

Figure 5: Visual appearance of GPM and PCM samples after 52 weeks of exposure to 0.352 mol/L solutions of a) Na_2SO_4 and b) $MgSO_4$.

3.2.2. pH of sulfate solution

The change in pH of Na_2SO_4 and $MgSO_4$ solution used for storing the GPM and PCM bar samples is shown in Figure 6. The pH values of fresh Na_2SO_4 and $MgSO_4$ solutions were around 6.9 and 7.4, respectively. When mortar samples were immersed in the solutions, the pH of the solutions increased, which is reflected by relatively high pH measured after the first week of the test. The increase in pH was caused by leaching of alkalis from the samples to the solutions.

For GPMs the pH of both sulfate solutions gradually decreased during the duration of the test, due to decreasing availability of basic ions that could be leached out from the samples. For Na_2SO_4 solution the pH decreased from above 11 to below 10, while for $MgSO_4$ solution it decreased from around 9.5 to below 8.

In comparison to results obtained for GPMs, pH of sulfate solutions used for PCM mixes was higher. For the first 28 weeks of the test, the pH of the Na_2SO_4 solution was above 12.5, while for $MgSO_4$ solution it was above 10. The pH of these two solutions decreased slightly (to around 12 and 9.5, respectively) by week 52. These trends are in good agreement with literature [78] and can be explained as follows. The initial Na_2SO_4 reaction with calcium hydroxide from hcp results in the formation of gypsum and sodium hydroxide. Consequently, due to high solubility of sodium hydroxide in water, the pH of hcp increases to above 13.5. Initially, the $MgSO_4$ attack on calcium hydroxide causes the formation of gypsum and magnesium hydroxide (brucite). This process continues until calcium hydroxide becomes depleted. As brucite is poorly soluble in water, its presence decreases the pH of the hcp to around 10.5.

Where strength grade is concerned, the Na_2SO_4 solution used to store GPM-60 samples had lower pH than that used for GPM-37.5. In all other cases, the pH of the

solutions was almost the same between mixes made from the same binder, but with different strength grade.

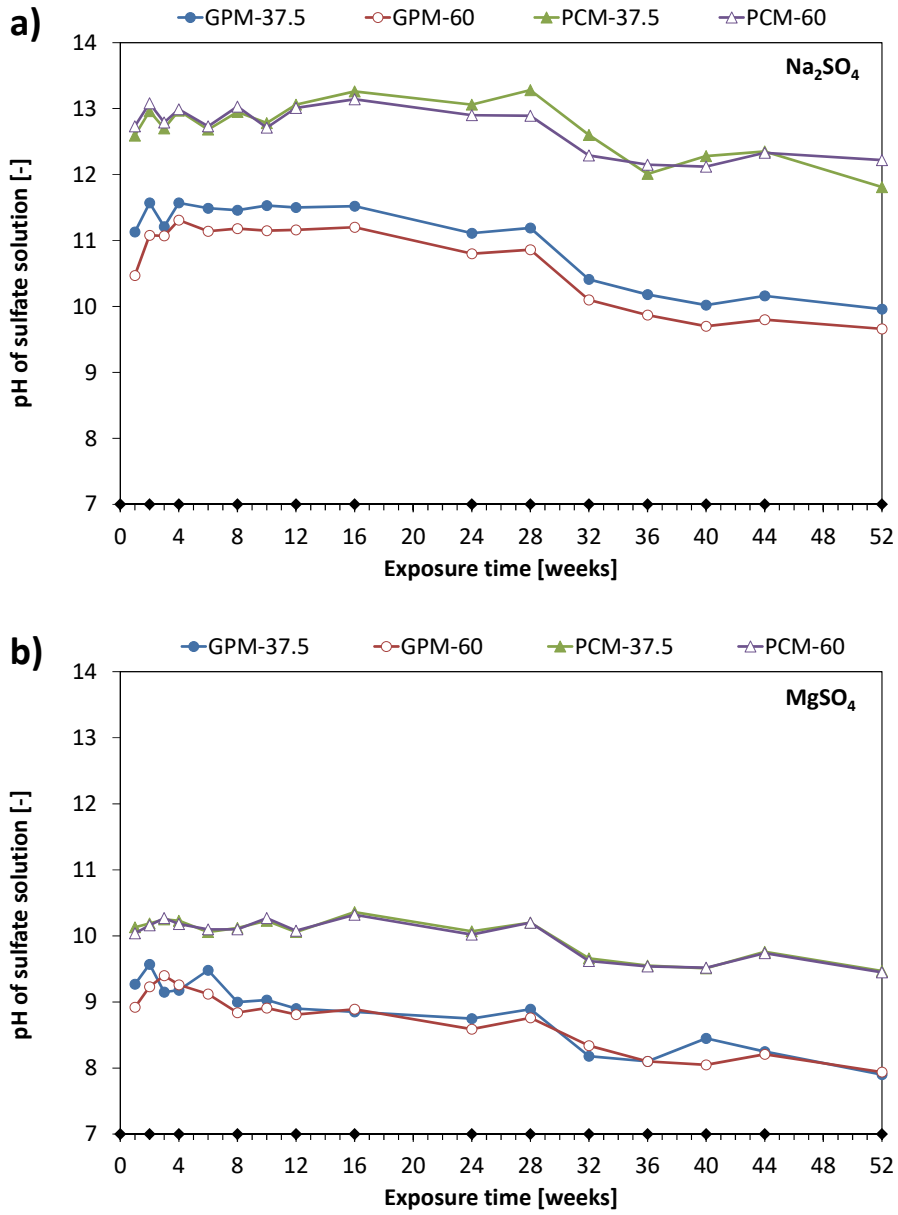

Figure 6: pH changes of a) Na_2SO_4 solution and b) $MgSO_4$ solution during 52 weeks of mortar bars immersion (diamonds represent time of solution replenishment).

3.2.3. Mass change

The mass change of GPM and PCM bar samples during 52 weeks of exposure to the solutions of Na_2SO_4 and $MgSO_4$ are shown in Figure 7. The mass of the GPM samples

increased slightly (to a maximum of 0.12% of their mass at 28-day) after being exposed to the sulfate solutions. Then it progressively decreased, reaching a minimum of -0.30% and -0.17% for Na_2SO_4 and $MgSO_4$, respectively. The initial mass gain is believed to be due to small absorption of the solution into the microstructure of the samples. The reason for the mass loss is not clear, but it was assumed that due to relatively frequent replenishment of the sulfate solution, significant leaching of alkalis from the GPM samples occurred. It is in agreement with the observed decrease in pH of solutions used for storing the samples (Figure 6).

Mass of PCM samples increased as a result of the sulfate attack, which was caused by sulfate uptake. In the case of Na_2SO_4 solution, the mass of samples increased gradually to 5.1% and 2.9% for PCM-37.5 and PCM-60, respectively. Measurements for PCM-37.5 stopped at week 24 as the samples fragmented. Mass of PCM-37.5 and PCM-60 stored in $MgSO_4$ solution increased steadily up to week 24 (reaching an increase in mass of 2.8% and 1.8%, respectively) and then the increase rate was lower for mix PCM-37.5 (reached 4.3% increase in mass at the end of the testing), while mix PCM-60 started to loose mass (at 52 weeks the mass increase was only 0.3%). For both PCM mixes stored in $MgSO_4$ solutions, crumbling of the edges was observed after week 24 (Figure 5), hence leading to changes in the initial trends. As a result, for mix PCM-60, the mass gain associated with sulfate uptake was offset by the mass loss related to edge crumbling.

The influence of compressive strength grade of GPMs on the samples' mass change was insignificant. PCM samples with higher strength showed lower mass change. As the porosity of the PCM-60 samples was lower than that of PCM-37.5, they accumulated less sulfate attack products.

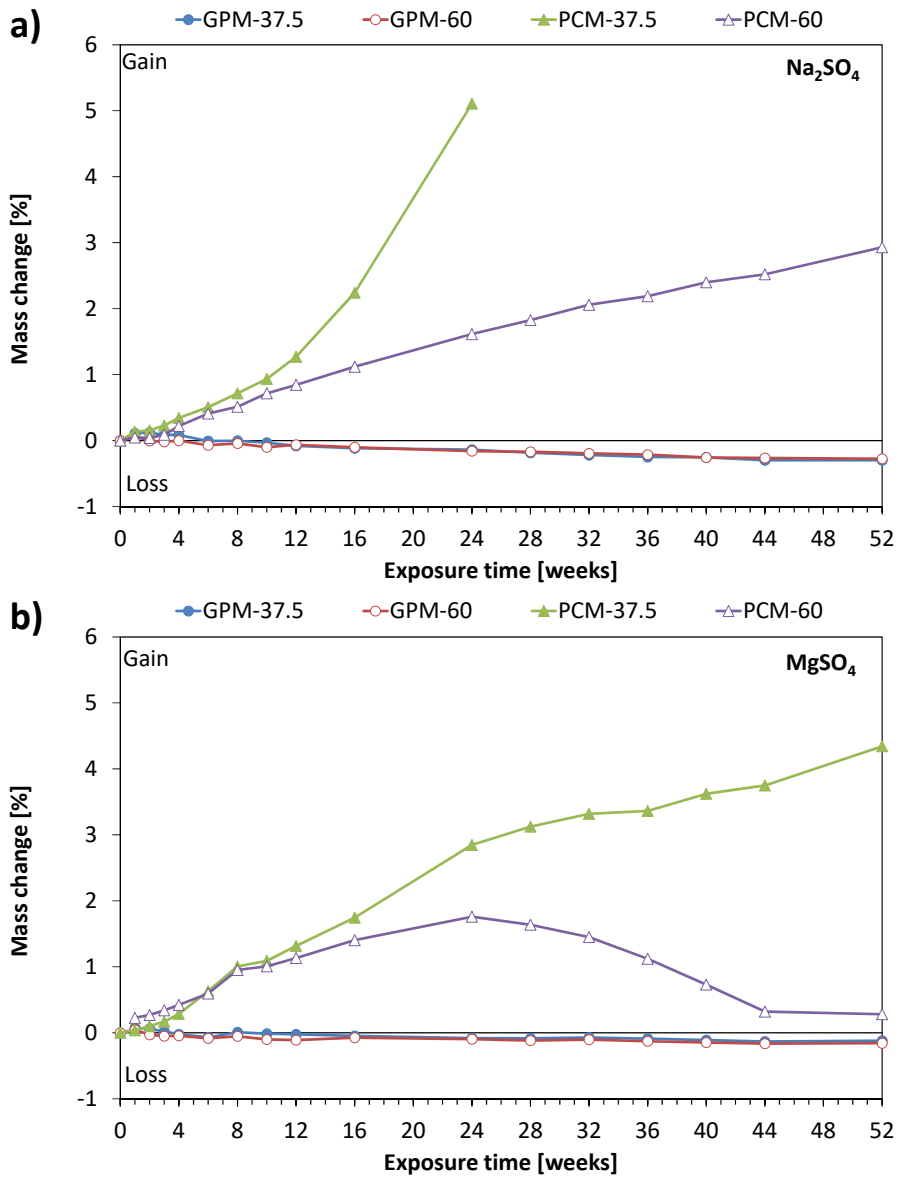

Figure 7: Mass change of GPM and PCM mixes exposed to a) Na_2SO_4 solution and b) $MgSO_4$ solution.

3.2.4. Length change

The length change of GPM and PCM bar samples exposed to the sulfate solutions are shown in Figure 8. The y-axes are set to length change of 5000 microstrain, and the enlarged portions of the graphs are showing the entire range of length change for mix PCM-37.5.

Regardless of strength grade, throughout the 52 weeks of testing, samples of GPMs proved to be stable in sulfate solutions, exhibiting relatively small change in length. GPM bars exposed to Na_2SO_4 showed minor shrinkage of less than 200 microstrain, while samples stored in $MgSO_4$ solution showed minor expansion not exceeding 200 microstrain. It is not

clear what caused the shrinkage of the samples stored in Na_2SO_4, but it was most probably related to relatively larger mass loss observed for Na_2SO_4 than for $MgSO_4$ (Figure 7).

As expected, PCM samples exposed to sulfate ions showed considerably larger expansion than similar GPM samples. This was due to transport of sulfate ions into hcp pore structure and then reaction with hcp to form expansive salts [79]. At the same age, PCM samples exposed to Na_2SO_4 had larger expansion than those stored in $MgSO_4$ solution. This was linked to the type of expansive salts formed, and is discussed in the section on XRD. Samples of mix PCM-37.5 immersed in Na_2SO_4 started disintegrating before week 28 of the test and for the last measurement at week 24 had expansion exceeding 20600 microstrain (shown in the enlarged graph). Expansion of PCM-60 reached nearly 4300 microstrain by the end of the test. For $MgSO_4$ solution, PCM-37.5 and PCM-60 mortar bars had expansion exceeding 15500 and 5900 microstrain, respectively. For all PCMs, expansion occurred in two stages, where 'induction' period characterized by low expansion value was followed by steady increase in expansion [80]. In the case of Na_2SO_4 attack the transition between these two stages occurred earlier and was sharper [80].

No influence of strength grade was observed for GPMs, while it was evident that higher strength PCM mixes had lower expansion. Lower expansion of PCM-60 can be attributed to relatively slower intake of sulfate ions caused by denser microstructure and lower content of pores, which are obviously related to lower w/c ratio of this mix [76].

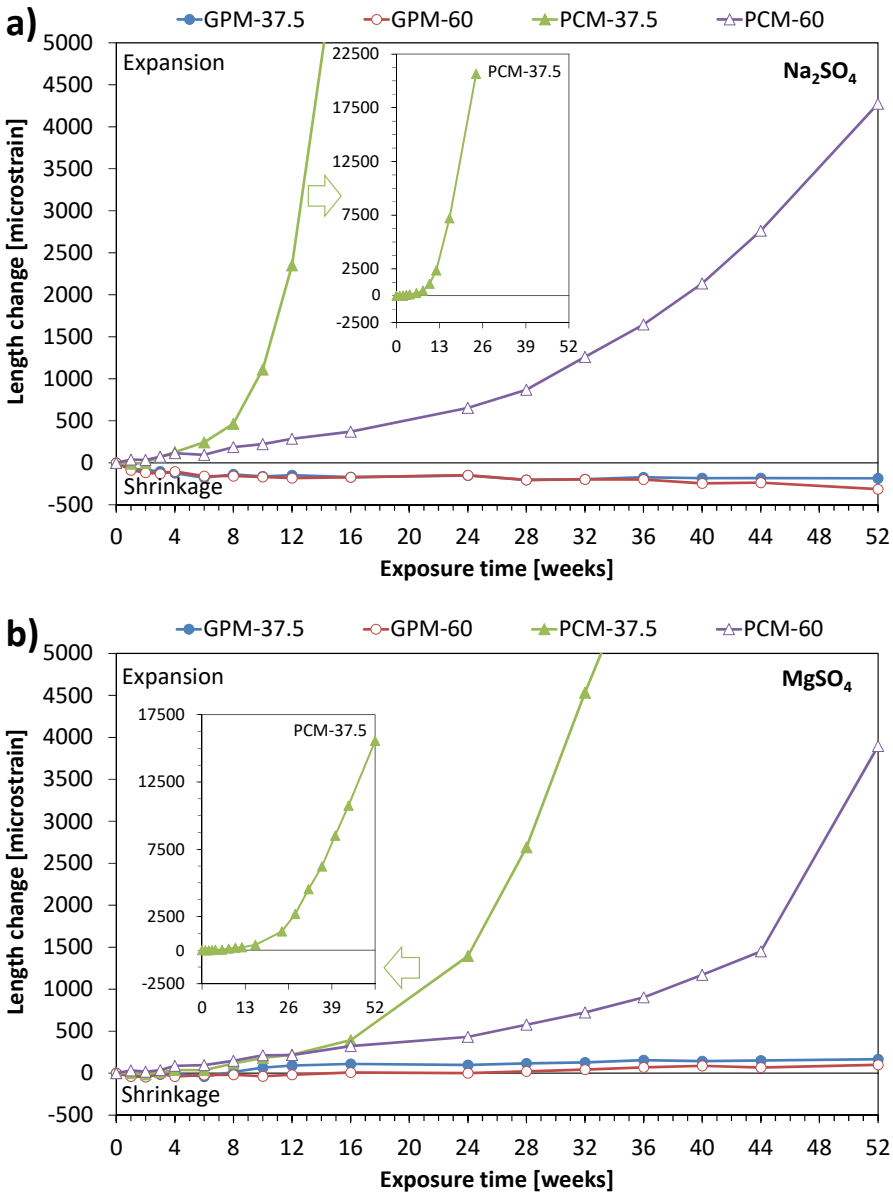

Figure 8: Length change of GPM and PCM mixes exposed to a) Na_2SO_4 solution and b) $MgSO_4$ solution.

3.2.5. XRD

Figure 9 shows the XRD spectra for the material collected from the outermost surface layer of GPM-60 and PCM-60, which were subjected to sulfate attack by Na_2SO_4 and $MgSO_4$. The spectra obtained from the center of the samples unexposed to sulfate attack (stored in water) are shown for comparison.

The main crystalline phase present in the control (unexposed) GPM-60 sample was hematite (H) with the main peaks observed at 2θ of 24.1, 33.2, 35.6 and 54.1°. In the

unexposed PCM-60, calcium hydroxide (CH) was identified by peaks at 2θ of 18.1, 28.7, 34.1, 47.1 and 50.8°. Both mortars contain quartz (Q), albite (AB), muscovite (M) and clinochlore (CL) due to the presence of sand (XRD pattern of sand is shown in Figure 2). The main quartz peaks are observed at 2θ of 20.9, 26.7, 36.6, 39.5, 42.5, 50.2 and 60.0°. The peaks at 2θ of 28.0 and 8.8° correspond to albite and muscovite, respectively. Finally, the peaks due to clinochlore are observed at 2θ of 6.3 and 12.5°.

After 52 weeks of either Na_2SO_4 or $MgSO_4$ attack, XRD patterns of the GPM-60 samples showed no significant change when compared with unexposed samples, proving the stability of the geopolymer mixes in sulfate environments.

For the PCM-60 samples, major changes to XRD patterns were observed. Calcium hydroxide (CH) was not present after exposure to both Na_2SO_4 and $MgSO_4$ solutions, which suggests its dissolution. Exposure of PCM-60 to Na_2SO_4 caused the formation of ettringite (E) and gypsum (G). Ettringite was observed by peaks at 2θ of 9.1, 15.8, 17.8, 18.9, 22.9, 32.4, 35.0 and 40.9°. The peaks at 2θ of 11.7, 20.7 and 29.2 are attributed to gypsum. Also calcite (C) was observed in the sample exposed to Na_2SO_4 by peaks at 2θ of 29.4, 36.0, 39.4, 43.2, 47.5 and 48.5°. Exposure to $MgSO_4$ resulted in the formation of an increased amount of gypsum highlighted by peaks at 2θ of 11.7, 20.7, 23.4, 29.2, 31.1, and 33.4°. Magnesium hydroxide, brucite (B), also formed, and resulted in peaks at 2θ of 18.6, 38.1, 50.9 and 58.7°. The above results for PCM exposed to both sulfate solutions are in good agreement with the literature [79]. Since ettringite is not stable below a pH of approximately 10.6, it was not detected in samples exposed to $MgSO_4$, but was present in samples exposed to Na_2SO_4. As discussed previously, the pH of sulfate solutions was governed by the products of sulfate attack reactions, i.e. sodium hydroxide and brucite, for Na_2SO_4 and $MgSO_4$ attacks, respectively. It is well known that ettringite occupies larger volume than gypsum [8]. As ettringite was predominantly detected in samples exposed to Na_2SO_4, this explained their

larger length change discussed in previous section. In addition, lower expansion of PCMs exposed to $MgSO_4$ may be attributed to the precipitation of brucite in the outmost surface layer of samples, which temporarily restricted penetration of Mg^{2+} into the pore structure [81]. As shown in Figure 5, a white precipitate formed on the outside of the PCMs exposed to $MgSO_4$. This precipitate was carefully collected and processed for XRD analysis as other samples. It was established that this layer mainly consisted of magnesium sulfate hydrate (MG) with peaks at 2θ of 16.3, 20.2, 22.0, 30.4 and 30.8°.

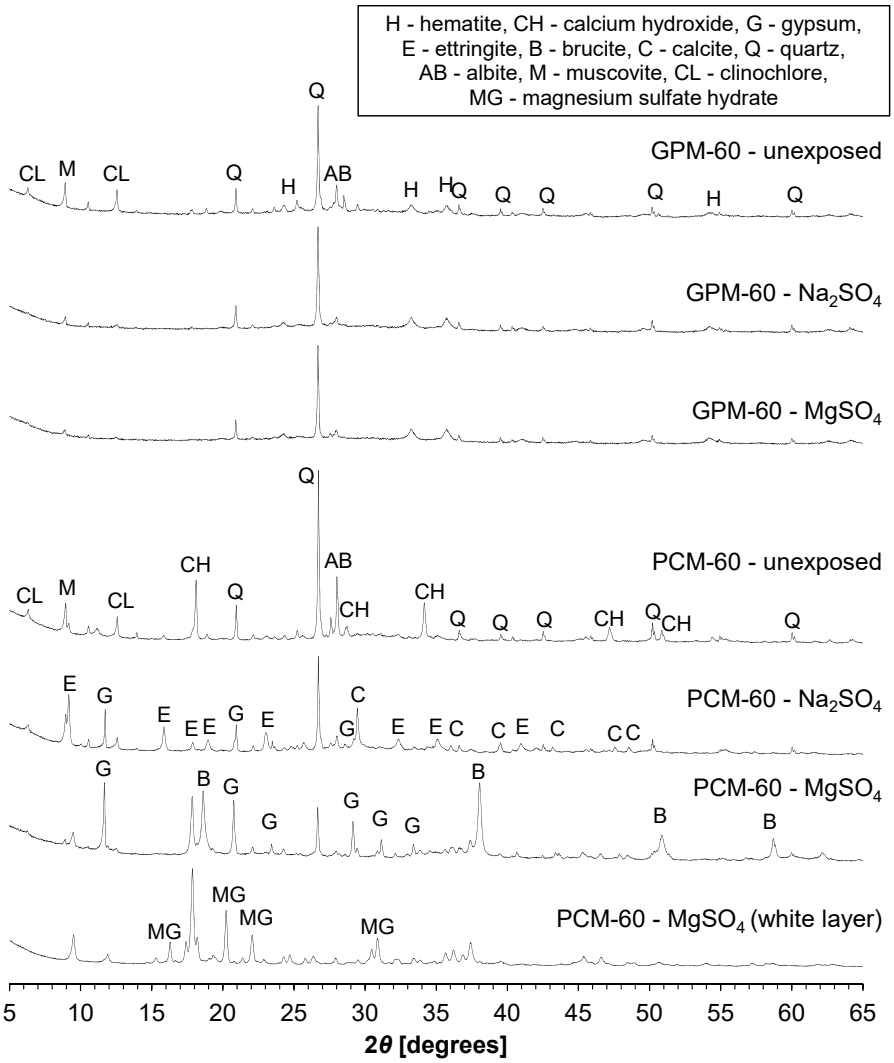

Figure 9: XRD patters of GPM-60 and PCM-60 control (unexposed) samples compared with samples exposed for 52 weeks to Na_2SO_4 and $MgSO_4$ solutions with concentration of 0.352 mol/L.

3.2.6. FTIR spectroscopy

Figure 10 shows the FTIR spectra for the outermost surface layer of GPM-60 and PCM-60 samples exposed to Na_2SO_4 and $MgSO_4$ solutions. They are compared to the spectra of inner section of the control (unexposed) samples, which were stored in water.

The unexposed sample of GPM-60 had a characteristic sharp band located at approximately 996 cm^{-1}, assigned to asymmetric T-O stretching (T = Si or Al), and a shoulder at approximately 860–890 cm^{-1}, related to M-O vibrations (M = K) [38]. The peak at approximately 1640 cm^{-1} and broad band centered at approximately 3400 cm^{-1} can be assigned to bending and stretching vibrations of water, respectively [38]. After the exposure of geopolymer samples to either of the sulphate solutions, there was very little change in the spectra, except for the main band located at around 996 cm^{-1}, which increased its intensity, but did not change the position.

In the case of both PCMs, intensity of a band observed in unexposed sample at 985 cm^{-1}, attributed to asymmetric Si-O stretching vibrations in C-S-H, reduced when samples were exposed to sulphate solutions [82]. A band at 3640 cm^{-1}, corresponding to O-H stretching vibrations in calcium hydroxide was not present in both samples exposed to sulfate solutions. The intensity of a broad shoulder near 1105 cm^{-1}, corresponding to asymmetric stretching vibrations of SO_4^{2-} in ettringite, became higher for samples stored in sulfate solutions [82, 83]. Presence of gypsum was detected in $MgSO_4$ sample, (shoulder at 1130 cm^{-1}, weak peak at 1620 cm^{-1} due to in plane bending vibrations of O-H···O group, and weak peak at 3405 cm^{-1} due to stretching vibrations of O-H [84, 85]. Presence of brucite ($Mg(OH)_2$) in a sample exposed to $MgSO_4$ solution was confirmed by a strong O-H vibration at 3694 cm^{-1} [86]. For samples exposed to Na_2SO_4 higher intensity of $CaCO_3$ was observed at wavenumber 874 cm^{-1} (out of plane bending of CO_3^{2-}), and broad band centered around 1412 cm^{-1} (asymmetric stretching of CO_3^{2-}).

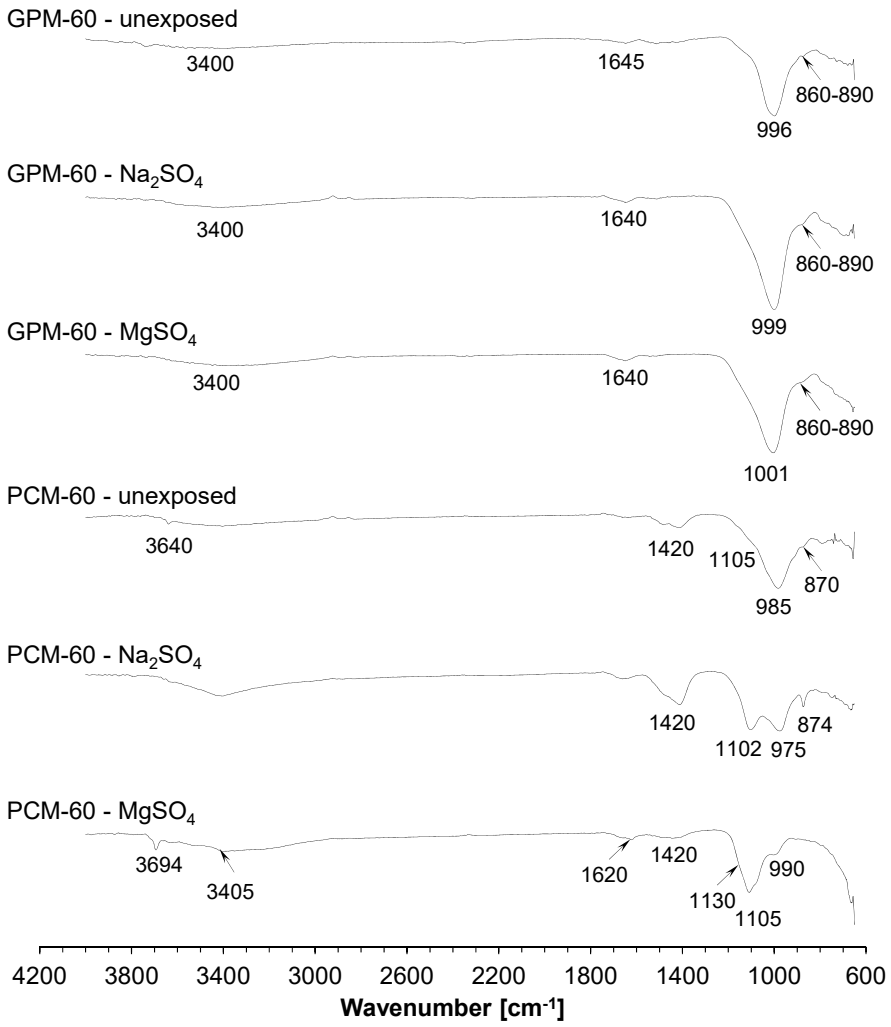

Figure 10: FTIR spectra of GPM-60 and PCM-60 control (unexposed) samples compared with samples exposed for 52 weeks to Na_2SO_4 and $MgSO_4$ solutions with concentration of 0.352 mol/L.

3.2.7. Summary for sulfate attack resistance

GPM mixes proved to be very stable in both Na_2SO_4 and $MgSO_4$ solutions during 52 weeks of immersion. Only small length and mass changes occurred, which are believed to be due to ion exchange between mortar samples and the sulfate solutions. Comparison of XRD and FTIR results for the material obtained from the outmost surface layer of samples exposed to the sulfate attack with that from the centre of the water cured samples revealed that no changes to the geopolymer microstructure occurred.

Sulfate attack by both Na_2SO_4 and $MgSO_4$ solutions caused visible deterioration, and large expansion of PCMs, making them unsuitable for use in sulfate rich environments. During the course of the test, samples exposed to Na_2SO_4 solutions progressively gained mass and expanded, which led to their expansive spalling and cracking. Although the mass gain and expansion of samples exposed to $MgSO_4$ solution was slightly lower than in those immersed in Na_2SO_4, they showed larger surface deterioration, which to some extent offset the mass gain. As confirmed by XRD and FTIR results, attack by both sulfate salts caused depletion of calcium hydroxide from the attacked portion of the samples. The presence of expansive salts was detected: gypsum and ettringite for Na_2SO_4 solutions, and gypsum for $MgSO_4$ for solutions. Samples attacked by $MgSO_4$ solution revealed the presence of brucite.

Strength grade had no influence on the results of sulfate attack on GPM samples. In contrast, high strength PCM mix showed lower degree of degradation and expansion than the normal strength mix. This was linked to lower porosity and denser microstructure of the former mix.

3.3 Resistance to acid attack

The resistance of PCM and GPM samples to acid attack is presented in this section. Description of the changes in visual appearance of samples immersed in H_2SO_4 and HCl solutions is followed by mass changes of samples, changes in the pH of acid solutions, microstructural changes of samples determined by XRD analysis and FTIR spectroscopy, and finally a summary of the findings is presented.

3.3.1. Visual appearance

The visual appearance of samples after 8 weeks of exposure to a range of solutions of H_2SO_4 and HCl acids are shown in Figure 11.

Regardless of the acid type and concentration, GPM samples showed less surface deterioration than the PCM samples. Where the strength class for the same binder type is concerned, mixes with lower strength had larger deterioration. PCM mixes showed relatively larger differences between the strength grades than GPMs.

In general, all samples exposed to H_2SO_4 solutions deteriorated more than those attacked by HCl solutions. This was particularly visible with higher acid concentrations, where part of the binder was removed from the surface layer and sand particles became exposed. For PCM mixes, the edges of samples exposed to H_2SO_4 solutions became rounded, while they were relatively well preserved in HCl solutions. However, the acid type did not have a significant effect on the edge deterioration of GPM samples. PCM samples exposed to H_2SO_4 acid solutions had white precipitation on the surface, while the surface of samples stored in the HCl solutions turned light brown in parts. The white precipitation was identified as gypsum (as discussed in the XRD section). The light brown discoloration is likely related to precipitation of loosely bound ferric hydrates at pH above 2 [87, 88]. In contrast, neither of these two acids resulted in a colour change of the GPM samples.

The degree of deterioration of all samples increased with the increase in the concentration of the acid solutions. The surface of sand particles became visible at high concentrations whilst at 0.10 mol/L of H_2SO_4 only GPM samples had small imperfections. No sand particles were detached from the GPM binder matrix. For PCMs exposed to 0.10 mol/L of H_2SO_4 solutions, parts of the samples lost an outer layer, exposing the surface of sand particles. At higher concentrations, a part of the hardened binder and some of the sand particles were removed. Similar pattern, but to a lesser extent, was observed for HCl solutions.

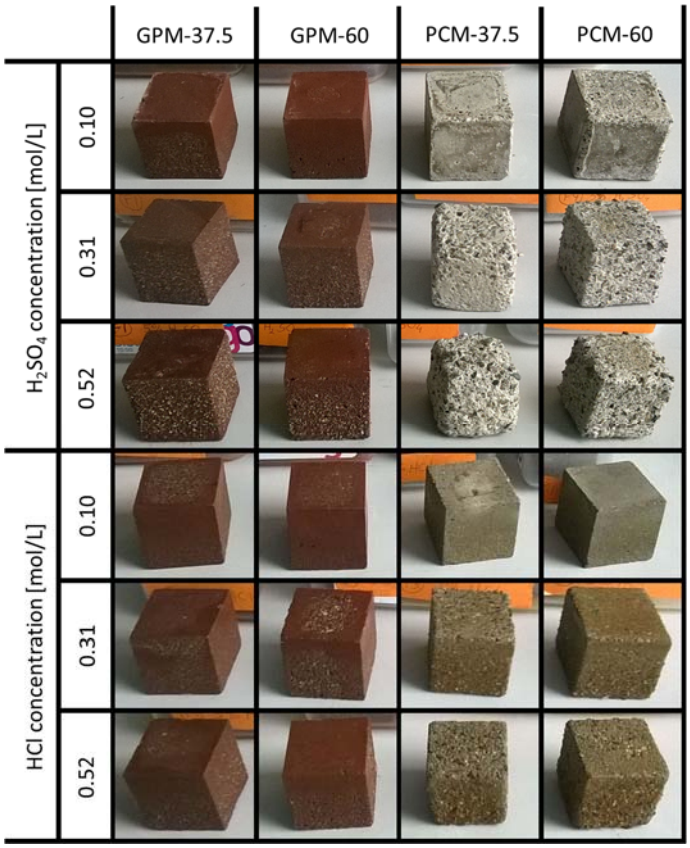

Figure 11: Visual appearance of GPM and PCM samples after 8 weeks of exposure to different H_2SO_4 and HCl acid solutions.

3.3.2. Mass change

Mass changes in mortar samples during 8 weeks of immersion in H_2SO_4 and HCl solutions are shown in Figure 12 and Figure 13, respectively. The rate of mass loss in GPM samples exposed to H_2SO_4 was decreasing from one cycle to the next during the 8 weeks of the test. Sample GPM-37.5 reached maximum mass loss of 2.4, 5.5 and 7.9% at week 8 when exposed to H_2SO_4 solutions with concentrations of 0.10, 0.31 and 0.52 mol/L, respectively. In contrast, PCM samples gained mass initially (except for PCM-60 immersed in 0.52 mol/L H_2SO_4 solution), and then they started to loose mass. In all cases, the mass gain was below 1.4% of the initial samples' mass. As evidenced by the colour change of the samples' surface, the mass gained was most probably related to decalcification of hcp and formation of a layer of sulfate rich salts, gypsum and ettringite [88], on the surface of samples. Most likely, these salts also formed in the pores of the outermost surface layer of the samples.

At this stage no degradation was observed. The mass loss was the result of a high degree of hcp decalcification and, most importantly, the result of progressive degradation of the surface layer caused by pressure exerted by expansive crystals of the salts formed inside the pore structure. The presence of gypsum was confirmed with XRD studies [8]. A layer-by-layer degradation of the sample surface caused by the expansive spalling offset the increase in mass [88]. At the end of the test, the maximum mass loss of 13.2 and 24.9% was recorded for PCM-60 exposed to solutions with concentrations of 0.31 and 0.52 mol/L, respectively.

When exposed to HCl solutions, the rate of mass loss of the GPM mixes during the 8 weeks of the test was decreasing from one cycle to the next during. At the end of the test the maximum mass loss observed for mix GPM-37.5 was 1.6, 3.6 and 5.5% for HCl concentrations of 0.10, 0.31 and 0.52 mol/L, respectively. The rate of mass loss of PCM samples exposed to HCl solutions was increasing from one cycle to the next, due to decalcification of the samples and, to a lesser extent, to release of aluminium and iron [88]. At the end of the test, the maximum mass loss was recorded for mix GPM-37.5, *i.e.* 1.3, 5.3 and 12.3% for HCl concentrations of 0.10, 0.31 and 0.52 mol/L, respectively.

Irrespective of the acid type, it appears that for GPM mixes the mass loss rate decreased during the course of the test (and in some cases stabilised somewhere between the third and the fifth week of the test), while for PCMs it accelerated. It also depended on the acid solution concentration; the decrease (GPMs) or increase (PCMs) in mass loss rate happened earlier for high acid concentrations. This suggests that the degraded layer of the material in GPM mixes acted as a buffer zone and slowed down further progression of the acid attack, thus providing better overall resistance against the acid attack than the PCM counterparts.

The higher strength GPM samples exposed to H_2SO_4 and HCl solutions and high strength PCM samples exposed to HCl solutions exhibited lower mass loss than the normal

strength mixes. It was most probably related to lower porosity of the high strength mix. For GPM mixes, the difference in the cumulative mass loss between high and normal strength mixes exposed to either acid type was not significant (up to 0.9%). In the case of PCM mixes exposed to HCl, the difference in the cumulative mass loss between high and normal strength mixes increased with exposure time. Moreover, mass loss of samples exposed to HCl increased with an increase in acid concentration (at 8 weeks exceeding 0.5, 1.1 and 2% for the HCl solution with concentration of 0.10, 0.31 and 0.52 mol/L, respectively – see Figure 13c and d). High strength PCMs exposed to H_2SO_4 solutions with concentrations of 0.31 and 0.52 mol/L showed higher mass loss than the normal strength mixes. Also, the difference in mass loss between strength classes was significantly higher. Rahmani and Ramazanianpour [24] attributed this behaviour to the difference in pore size. Specifically, for low w/c ratio (mix PCM-60) the ingress of H_2SO_4 acid is hindered to some extent by lower porosity and pore size of the matrix, hence the acid reacts with hcp in the outermost surface layer of the sample. Decalcification of the hcp is accompanied by build-up of expansive salts in the acid degraded zone. As the pores of the high strength mix are comparatively smaller (Table 3), the pressure exerted by the expansive salts leads to relatively quicker degradation of the surface and advances the acid attack front deeper into the matrix. In the case of higher w/c ratio, due to more porous hcp, acid is able to penetrate deeper into the hcp. However, pressure related to build-up of the expansive salts is relatively lower due to the more porous matrix. The expansive products form a layer on the acid attack front, which to some extent decreases the degree of the attack. Also, as the PCM-60 contained more cement (Table 2), there were more cement hydration products to react with H_2SO_4.

Where acid type is concerned, GPMs exposed to all three concentrations of H_2SO_4 and PCM mixes immersed in 0.31 and 0.52 mol/L solutions of H_2SO_4 lost relatively more mass than comparable mixes stored in HCl solutions. In contrast, PCM samples exposed to

0.10 mol/L H_2SO_4 solution gain mass, while mass loss was observed for the samples stored in corresponding solution of HCl.

Irrespective of the binder and acid types, an increase in acid solution concentration caused greater mass change [11, 88].

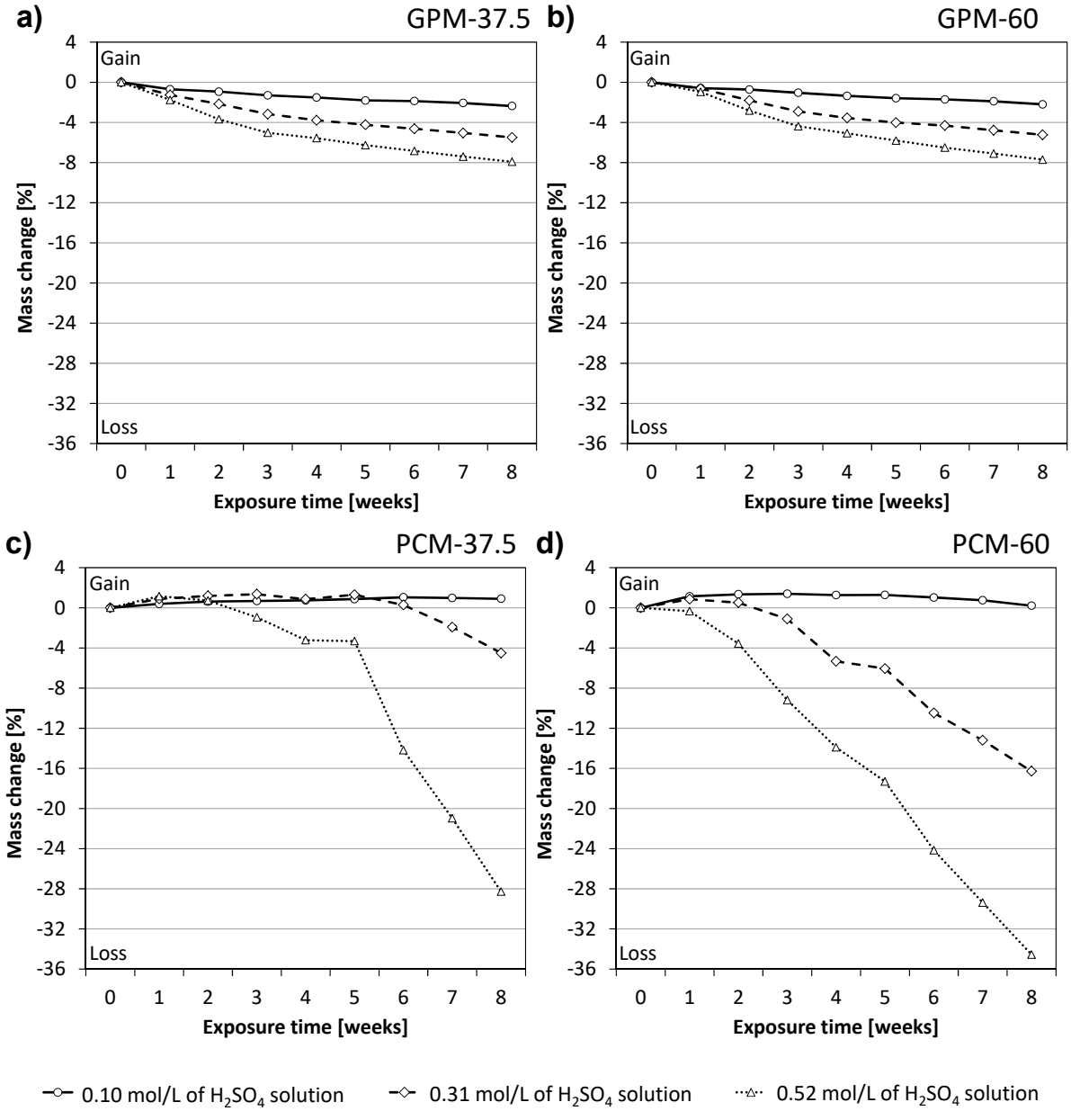

Figure 12: Mass loss of GPM and PCM mixes exposed to different concentrations of H_2SO_4 solutions over a period of eight weeks.

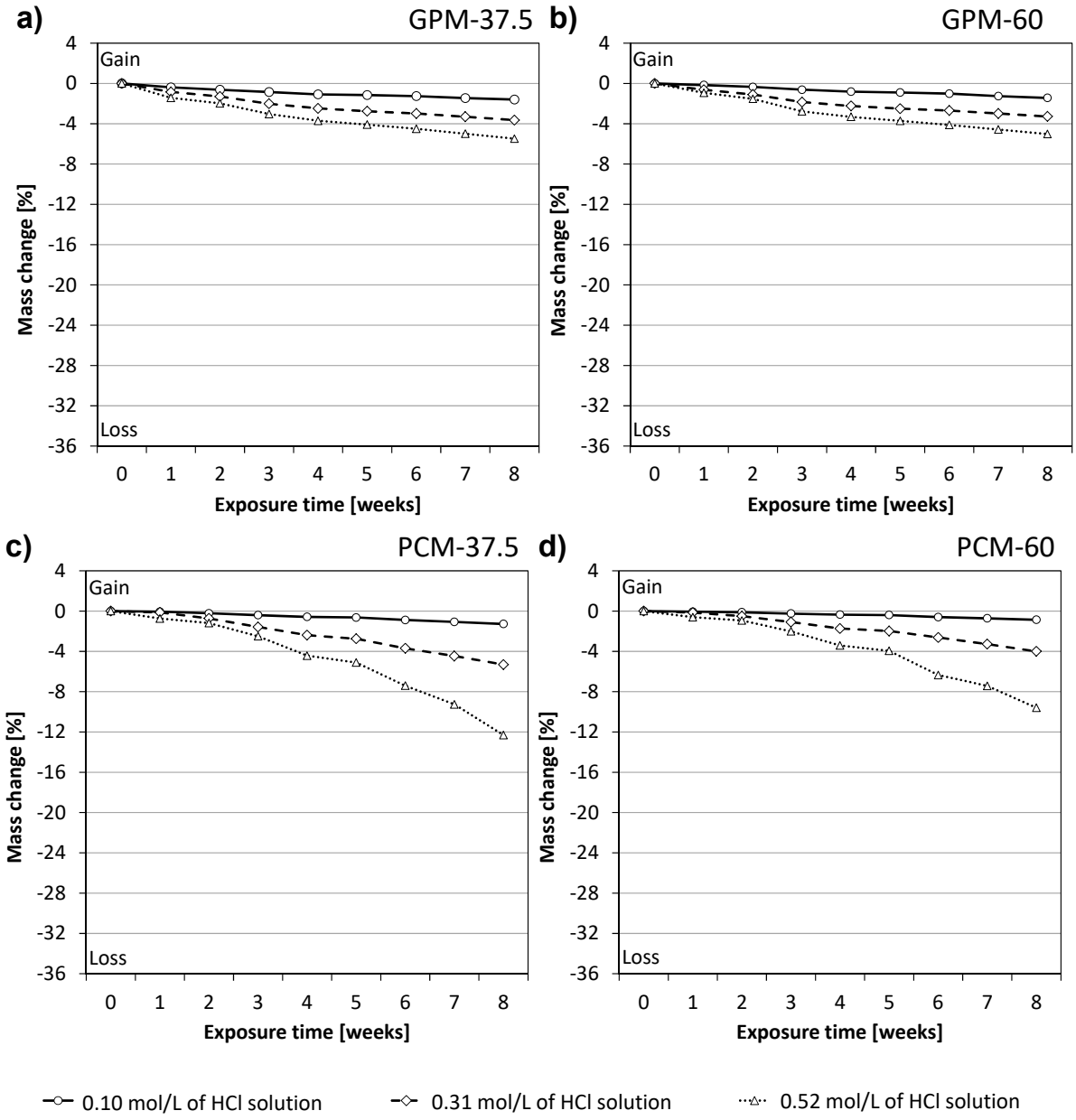

Figure 13: Mass loss of GPM and PCM mixes exposed to different concentrations of HCl solutions over a period of eight weeks.

3.3.3. Acid solution pH

An example of the pH profiles of the acid solutions during 8 weeks of the test for high strength mortar mixes are shown in Figure 14 for H_2SO_4 and in Figure 15 for HCl. Very similar trends were obtained for normal strength mixes. During each of the weekly cycles, the pH increased from the level recorded for the replenished solution due to dissolution of highly alkaline binders.

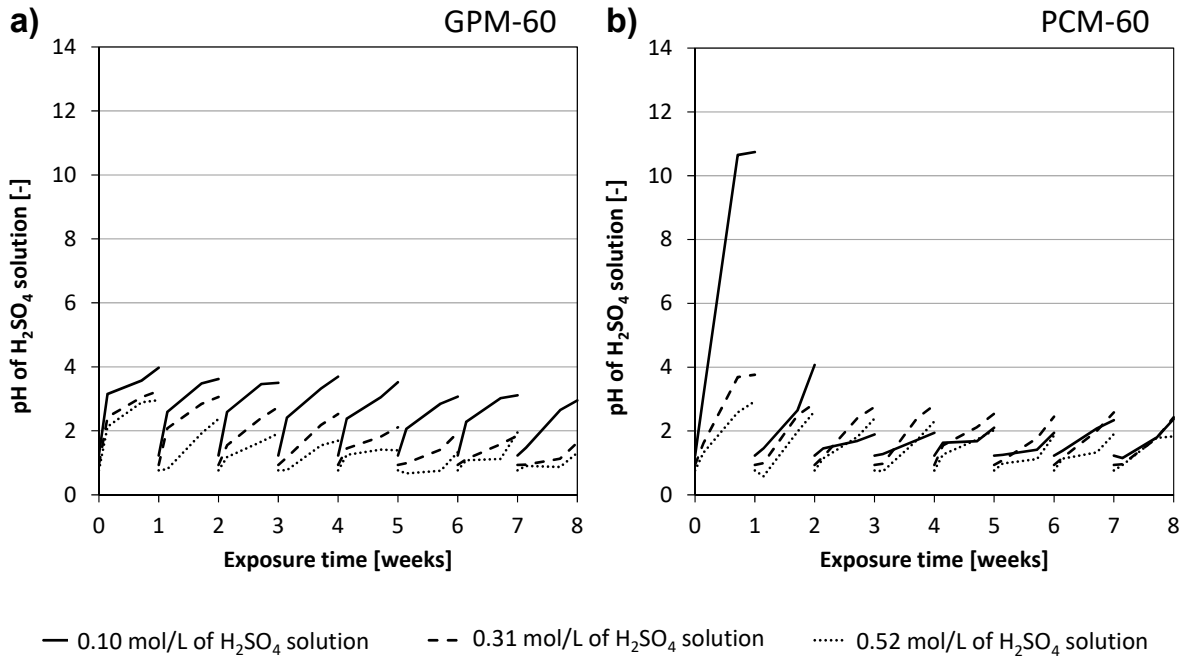

Figure 14: pH changes of H_2SO_4 solutions with different concentrations over a period of eight weeks.

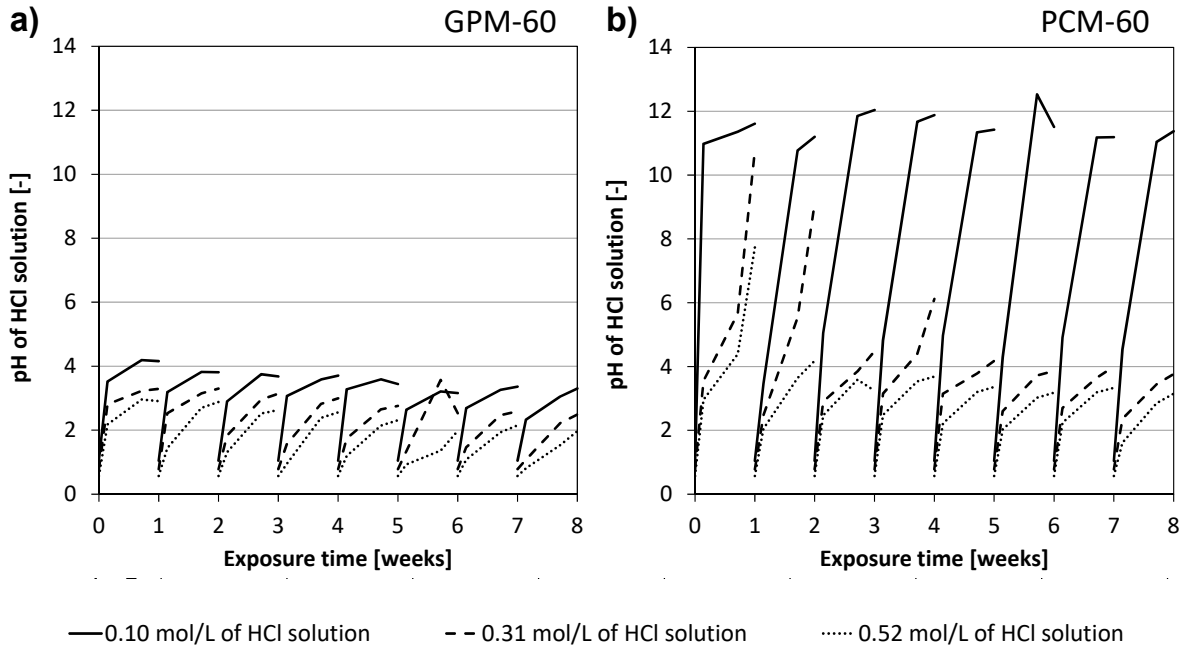

Figure 15: pH changes of HCl solutions with different concentrations over a period of eight weeks.

In most cases, the weekly increase in pH was smaller every consecutive week, as shown in graphs of the pH of solutions measured before replenishing with a fresh solution (Figure 16). This observation holds true for all combinations but PCMs immersed in 0.10

mol/L HCl and 0.10 mol/L of H_2SO_4. Typically, the pH values were the highest before the first renewal of the solutions, due to the outermost layer of the samples being attacked by the acids. Subsequently, the acid had to diffuse through the already degraded layer to react with the unattacked material, which resulted in smaller increases in pH over the subsequent weeks. Importantly, pH of solutions in which GPM mixes were immersed were in general lower than the PCM counterparts, which likely resulted from lower pH of the geopolymer mortars and/or the lower reaction with/dissolution of material from the specimens.

The strength grade of GPMs exposed to both H_2SO_4 and HCl solutions, and PCMs exposed to HCl solutions, did not have a significant effect on the pH (Figure 16). In contrast, high strength PCMs samples immersed in 0.31 and 0.52 mol/L H_2SO_4 solutions, caused the pH to be higher than normal strength PCMs. This could be related to higher degradation rate of high strength PCMs, as already mentioned in the section on mass change. The pH of the 0.10 mol/L H_2SO_4 solution used for PCM-60 was initially lower than that for PCM-37.5, but after the fourth replenishment of the solution it became higher. This correlated well with the mass change results. For PCM-37.5, there was a constant increase in mass until week six of the test (Figure 12c), while for PCM-60 the mass gain stopped after week four (Figure 12d). This corroborates with changes in the pH trends for these samples, supporting the hypothesis that the acid started penetrating the protective layer of the precipitated salts, on the surface or inside the outermost layer of the samples.

Regardless of the strength grade of either GPM or PCM mixes, the post-immersion H_2SO_4 solutions had slightly lower pH than the corresponding HCl solutions (Figure 16). The discrepancy was much larger for PCM samples, especially for those stored in 0.10 mol/L solutions. In the first 3 weeks of the exposure, the pH of 0.10 mol/L H_2SO_4 solution dropped below 3, while for HCl solution it almost did not change during the 8 weeks of testing.

Using acid solutions with higher concentration caused lower rise in acid solutions pH, with the exception of PCM samples immersed in 0.10 mol/L of H_2SO_4 solution, as discussed above.

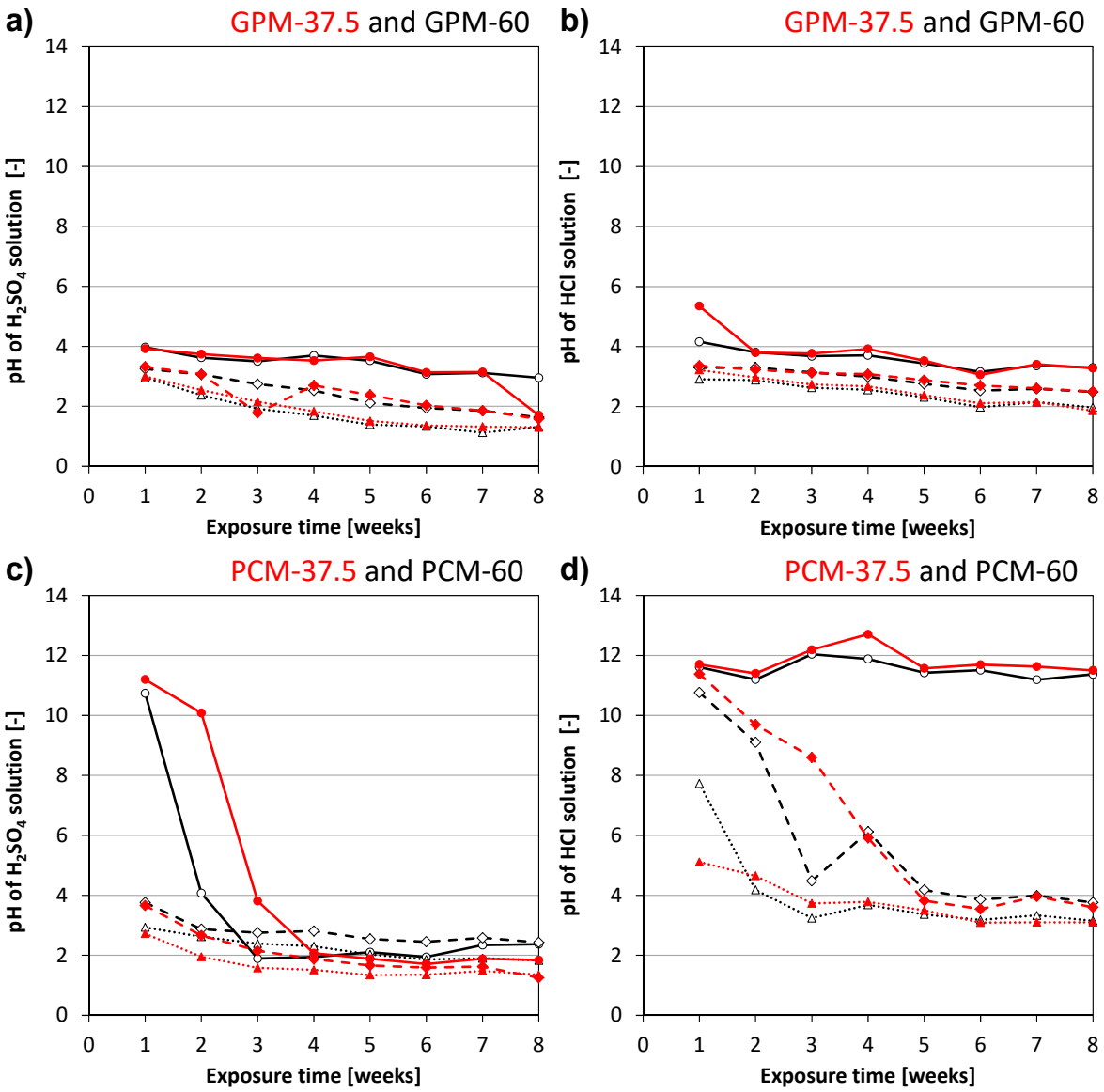

Figure 16: Influence of binder type and strength grade on evolution of pH values of H_2SO_4 and HCl acid solutions with different concentrations over a period of eight weeks (measurements made before replenishing with a fresh solution).

3.3.4. XRD

The XRD patterns of the materials collected from the center of unexposed GPM-60 and PCM-60 samples are compared with the patterns recorded for the degraded layer, collected from samples exposed for 8 weeks to H_2SO_4 and HCl solutions (0.52 mol/L) in Figure 17. The unexposed samples used in acid attack testing (Figure 17) have very similar XRD patterns to the unexposed samples used for sulfate attack Figure 9, hence, the discussion of their XRD results is not repeated here.

Very little change upon the acid attack was observed in GPM-60, particularly for HCl acid attack, which is in agreement with results reported by Bouguermouh *et al.* [39] for metakaolin based geopolymers. Following the H_2SO_4 attack, a small peak corresponding to gypsum was identified at 2θ of 11.7° in the XRD pattern, revealing that calcium in the calcined lithomarge reacted with H_2SO_4 to form gypsum.

The XRD patterns of the PC mortars showed greater changes after acid attack. Calcium hydroxide was no longer identified after attack by either HCl or H_2SO_4, suggesting it had reacted with the respective acid. After H_2SO_4 attack, gypsum was identified by peaks at 2θ of 11.7, 20.7, 23.4, 29.2, 31.1, 33.4 and 43.3°.

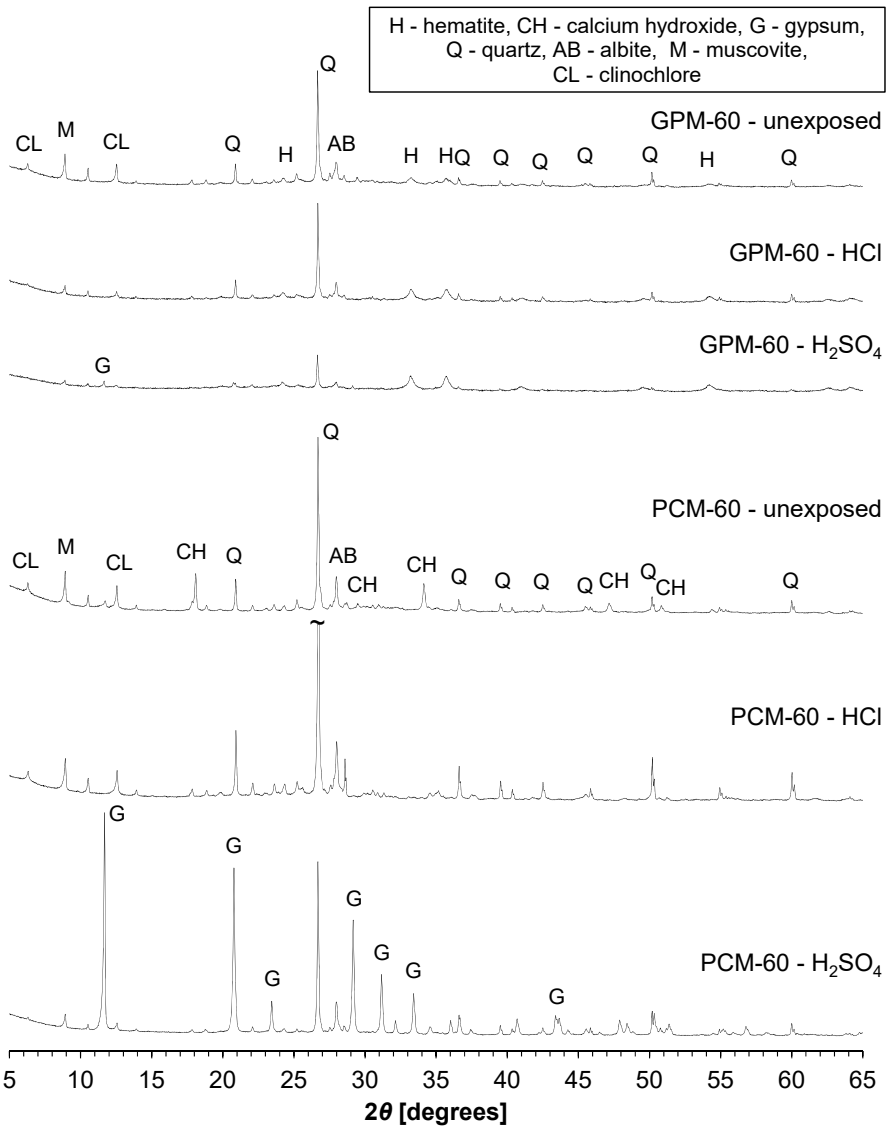

Figure 17: XRD patterns of GPM-60 and PCM-60 control (unexposed) samples compared with samples exposed for 8 weeks to HCl and H_2SO_4 solutions with concentration of 0.52 mol/L.

3.3.5. FTIR spectroscopy

Figure 18 shows the FTIR spectra of the material deteriorated from GPM-60 and PCM-60 samples subjected to acid attack in 0.52 mol/L solutions of HCl or H_2SO_4. The spectra obtained from the centre of control samples, not exposed to acid attack, are also shown.

For the unexposed geopolymer sample the main peak was at 996 cm^{-1} (asymmetrical T-O vibrations, where T = Si or Al [38]). It shifted to 1036 and 1044 cm^{-1} after HCl and H_2SO_4 acid attacks, respectively, suggesting that acid attack caused an increase in the Si/Al

ratio due to the removal of aluminium from the binder [36]. Bernal *et al.* [37] reported that the extent of the shift to higher wavenumbers can be related to the degree of structural damage to the binder. In this case, H_2SO_4 acid caused a larger shift of the peak and also caused a larger mass loss than HCl (Figure 12a,b and Figure 13a,b, respectively). Of notice is that the FTIR spectrum for the unreacted calcined lithomarge featured a strong signal at 1036 cm^{-1}, similarly to acid attacked samples. It suggests that, in addition to the degraded (dealuminated) binder and sand, the corroded samples contained unreacted calcined lithomarge particles [36]. A shoulder at 900–980 cm^{-1} appeared for samples attacked by either acid, which can be attributed to the removal of K^+ ions and the incorporation of H_3O^+ ions in the degraded structure [36]. This suggests that dealumination of the binder is the main mechanism of failure of GPM to acid attack. In contrast to XRD results, gypsum was not found in GPM-60 sample attacked by H_2SO_4. No further significant changes to the FTIR spectra were observed.

In the case of the PCMs, the main peak was centred at 985 cm^{-1} and shifted to 1039 cm^{-1} after the HCl attack, likely due to decalcification of C-S-H gel formed in Portland cement systems [37]. A band at approximately 3640 cm^{-1}, corresponding to O-H stretching vibrations in calcium hydroxide, was not present in samples exposed to the acid attack. Also, a peak at 870 cm^{-1} (out of plane bending of CO_3^{2-}) and a broad band at approximately 1420 cm^{-1} (asymmetric stretching of CO_3^{2-}), both corresponding to $CaCO_3$, were absent from the FTIR spectra of acid attacked samples. A broad shoulder near 1105 cm^{-1}, corresponding to asymmetric stretching vibrations of SO_4^{2-} in ettringite, was no longer present in acid attacked samples. The degraded material after sulphuric acid attack was mainly gypsum, with a very strong signal at 1115 cm^{-1} [89]. Further peaks at approximately 669 (the bending vibration of the SO_4 tetrahedron), 1620, 1685, (both in plane bending vibrations of O-H···O group), 3405

and 3536 cm^{-1} (both the stretching vibrations of O-H···O group) can also be related to the presence of gypsum [84, 85].

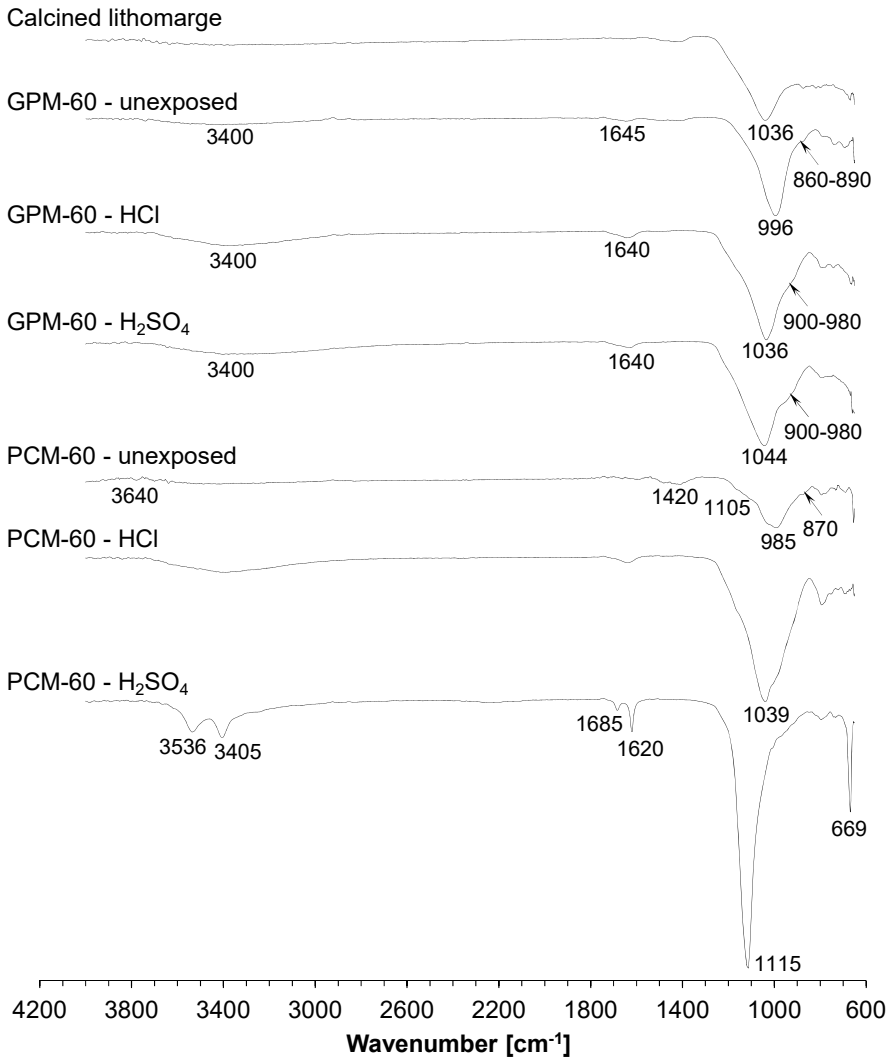

Figure 18: FTIR spectra of GPM-60 and PCM-60 control (unexposed) samples compared with samples exposed for 8 weeks to HCl and H_2SO_4 solutions with concentration of 0.52 mol/L.

3.3.6. Summary for acid attack resistance

In general, GPMs showed better resistance to attack by H_2SO_4 and HCl than PCMs (lower surface deterioration and lower mass loss), in particular to higher concentrations of these acid solutions, *i.e.* 0.31 and 0.52 mol/L. The rate of mass loss of GPMs decreased, while of PCMs increased, during eight weeks of the acid testing. This suggests that GPM

mixes provided a better quality (lower permeability) of acid-degraded layer, which restricted to some extent the diffusion of acid into the microstructure, hence lowering the degree of deterioration.

XRD results did not show any major changes to geopolymer microstructure caused by acid solutions. Based on FTIR spectroscopy results, dealumination of the geopolymer hardened binder accounted for the main mechanisms of the matrix deterioration of GPMs in both acids, with higher degree of changes detected for H_2SO_4. Also, FTIR spectra suggests that in the degraded matrix, K^+ ions were substituted with H_3O^+ ions.

Where PCMs are concerned, both acids had a dissolution effect on hcp caused by hydrogen ions (primarily dissolution of calcium hydroxide and decalcification of C-S-H and ettringite). In addition, H_2SO_4 acid caused precipitation of gypsum on the samples' surface and within pores of the already degraded near-surface layer, leading to expansive spalling caused by induced tensile stresses.

Due to their lower porosity, the high strength grade GPM samples exposed to solutions of both acids and high strength PCM samples exposed to HCl solutions, exhibited lower mass loss than the normal strength mixes. The opposite trend was observed for PCMs exposed to H_2SO_4 solutions with concentrations of 0.31 and 0.52 mol/L, which was attributed to faster build-up of expansive salts in less porous mixes causing expansive spalling.

Irrespective of the binder type and strength grade, solutions of H_2SO_4 induced more surface degradation and mass loss than the corresponding HCl solutions. The exception to this trend were PCM samples exposed to 0.10 mol/L H_2SO_4 solution which gained mass due to the precipitation of gypsum in the outermost surface layer of the samples.

For both binders, exposure to acid with a higher concentration caused a higher degree of surface deterioration and mass loss.

4. CONCLUSIONS

On the basis of the presented results, the following conclusions have been drawn:

- Irrespective of the sulfate solution used (Na_2SO_4 and $MgSO_4$) and the mortars' strength grade (37.5 and 60 MPa), GPM mixes showed superior sulfate resistance when compared with PCM mixes. No changes to the geopolymer microstructure were detected. Sulfate attack by both Na_2SO_4 and $MgSO_4$ solutions caused visible deterioration, and large expansion of PCMs, making them unsuitable for the use in sulfate rich environments.
- GPMs showed better resistance to attack by H_2SO_4 and HCl solutions than PCMs, *i.e.* lower surface deterioration and lower mass loss. Main mechanism of GPM deterioration was dealumination of the geopolymer microstructure. H_2SO_4 solutions caused higher degree of surface deterioration, mass loss and microstructural changes than corresponding HCl solutions. Due to lower microstructure porosity high strength GPMs performed better than normal strength ones.

Sulfate and acid attack on concrete structures is of great concern, in particular for wastewater transport and treatment infrastructure and agricultural applications. The currently used measures to minimise/reduce such deterioration are costly and in many cases require periodic renewal. This work has allowed greater understanding of the performance of a commercial geopolymer binder system in harsh sulfate and acid environments and will assist in the design of alternative concrete solutions. By using these more resistant geopolymer materials, maintenance costs will be reduced and service life increased.

ACKNOWLEDGEMENTS

The work reported here is a part of an ongoing Invest Northern Ireland funded collaborative research project (Ref. No.: RDO212970 – Development and commercialisation of banahCEM

geopolymer binder) between Queen's University Belfast and banah UK Ltd. The authors are grateful to the Invest Northern Ireland for the financial support and to the School of Natural and Built Environment for provided facilities.

REFERENCES

1. P.K. Mehta, and P.J.M. Monteiro, "Concrete: microstructure, properties, and materials", 3rd ed., McGraw-Hill, New York, USA, 2006, 659 pp.

2. P.A.M. Basheer, S.E. Chidiact and A.E. Long, "Predictive models for deterioration of concrete structures", *Construction and Building Materials*, Vol. 10, No. 1, 1996, pp. 27–37.

3. V. Živica, "Experimental principles in the research of chemical resistance of cement based materials", *Construction and Building Materials*, Vol. 12, No. 6-7, 1998, pp. 365–371.

4. M. Santhanam, M.D. Cohen, and J. Olek, "Sulfate attack research — whither now?" *Cement and Concrete Research,* Vol. 31, No. 6, 2001, pp. 845–851.

5. RILEM TC 211 – PAE, "Performance of Cement-Based Materials in Aggressive Aqueous Environments, State-of-the-Art Report, RILEM TC 211 – PAE", Eds, M. Alexander, A. Bertron, and N. De Belie, Vol .10, 2013, 462 pp.

6. J. Marchand, I. Older, and J.P. Skalny, "Sulfate Attack on Concrete", CRC Press, 2003, 232 pp.

7. R. Tixier, and B. Mobasher, "Modeling of damage in cement-based materials subjected to external sulfate attack, I: Formulation", *ASCE Journal of Materials in Civil Engineering*, Vol. 15, No. 4, 2003, pp. 305–322.

8. J. Monteny, E. Vincke, A. Beeldens, N.De Belie, L. Taerwe, D. Van Gemert, and W. Verstraete, "Chemical, microbiological, and in situ test methods for biogenic sulfuric acid corrosion of concrete", *Cement and Concrete Research*, Vol. 30, No. 4, 2000, pp. 623–634.

9. P.J.M. Monteiro, and K.E. Kurtis, "Time to failure for concrete exposed to severe sulfate attack", *Cement and Concrete Research*, Vol. 33, No. 7, 2003, pp. 987–993.

10. V. Zivica, and A. Bajza, "Acidic attack of cement based materials — a review: Part 1. Principle of acidic attack", *Construction and Building Materials*, Vol. 15, No. 8, 2001, pp. 331–340.

11. V. Zivica, and A. Bajza, "Acidic attack of cement-based materials — a review: Part 2. Factors of rate of acidic attack and protective measures", *Construction and Building Materials*, Vol. 16, No. 4, 2002, pp. 215–222.

12. R.E. Beddoe, H.W. Dorner, "Modelling acid attack on concrete: Part I. The essential mechanisms", *Cement and Concrete Research*, Vol. 35, No. 12, 2005, pp. 2333–2339.

13. ACI Committee 515, "ACI 515.2R-13 - Guide to Selecting Protective Treatments for Concrete Reported", *American Concrete Institute*, Farmington Hills, Michigan, USA, 2013, 25 pp.

14. A.A. Almusallam, F.M. Khan, S.U. Dulaijan, and O.S.B. Al-Amoudi, "Effectiveness of surface coatings in improving concrete durability", *Cement and Concrete Composites*, Vol.

25, No. 4–5, 2003, pp. 473–481.

15. J.B. Aguiar, A. Camões, and P.M. Moreira, “Coatings for concrete protection against aggressive environments”, *Journal of Advanced Concrete Technology*, Vol. 6, No. 1, 2008, pp. 243–250.

16. W. Tahri, Z. Abdollahnejad, J. Mendes, F. Pacheco-Torgal, and J. Barroso de Aguiar, “Cost efficiency and resistance to chemical attack of a fly ash geopolymeric mortar versus epoxy resin and acrylic paint coatings”, *European Journal of Environmental and Civil Engineering*, Vol. 21, No. 5, 2017, pp. 555–571.

17. E.F. Irassar, A. Di Maio, and O.R. Batic, “Sulfate attack on concrete with mineral admixtures”, *Cement and Concrete Research*, Vol. 26, No. 1, 1996, pp. 113–123.

18. M.A. González, and E.F. Irassar, “Ettringite formation in low C_3A Portland cement exposed to sodium sulfate solution”, *Cement and Concrete Research*, Vol. 27, No. 7, 1997, pp. 1061–1072.

19. E.F. Irassar, “Sulfate attack on cementitious materials containing limestone filler — A review”, *Cement and Concrete Research*, Vol. 39, No. 3, 2009, pp. 241–254.

20. E.K. Attogbe, and S.H. Rizkalla, “Response of Concrete to Sulfuric Acid Attack”, *ACI Materials Journal*, Vol. 85, No. 6, 1988, pp. 481–488.

21. C. Shi, and J.A Stegemann, “Acid corrosion resistance of different cementing materials”, *Cement and Concrete Research*, Vol. 30, No. 5, 2000, pp. 803–808.

22. J. Monteny, N. De Belie, and L. Taerwe, “Resistance of different types of concrete mixtures to sulfuric acid”, *Materials and Structures*, Vol. 36, No. 4, 2003, pp. 242–249.

23. E. Hewayde, M.L. Nehdi, E. Allouche, and G. Nakhla, “Using concrete admixtures for sulphuric acid resistance”, *Proceedings of the Institution of Civil Engineers - Construction Materials*, Vol. 160, No. 1, 2007, pp. 25–35.

24. H. Rahmani, and A.A. Ramazanianpour, “Effect of binary cement replacement materials on sulfuric acid resistance of dense concretes”, *Magazine of Concrete Research*, Vol. 60, No. 2, 2008, pp. 145–155.

25. F. Pacheco-Torgal, and Said Jalali, “Sulphuric acid resistance of plain, polymer modified, and fly ash cement concretes”, *Construction and Building Materials*, Vol. 23, No. 12, 2009, pp. 3485–3491.

26. O. Oueslati, and J. Duchesne, “The effect of SCMs and curing time on resistance of mortars subjected to organic acids”, *Cement and Concrete Research*, Vol. 42, No. 1, 2012, pp. 205–214.

27. A. Palomo, M.T. Blanco-Varela, M.L. Granizo, F. Puertas, T. Vazquez, and M.W. Grutzeck, “Chemical stability of cementitious materials based on metakaolin”, *Cement and Concrete Research*, Vol. 29, No. 7, 1999, pp. 997–1004.

28. T. Bakharev, J.G. Sanjayan, and Y.-B. Cheng, “Sulfate attack on alkali-activated slag concrete”, *Cement and Concrete Research*, Vol. 32, No. 2, 2002, pp. 211–216.

29. T. Bakharev, “Durability of geopolymer materials in sodium and magnesium sulfate solutions”, *Cement and Concrete Research*, Vol. 35, No. 6, 2005, pp. 1233–1246.

30. A. Fernandez-Jimenez, I. García-Lodeiro, and A. Palomo, “Durability of alkali-activated fly ash cementitious materials”, *Journal of Materials Science*, Vol. 42, No. 9, 2007, pp. 3055–3065.

31. V. Sata, A. Sathonsaowaphak, and P. Chindaprasirt, “Resistance of lignite bottom ash geopolymer mortar to sulfate and sulfuric acid attack”, *Cement and Concrete Composites*, Vol. 34, No. 5, 2012, pp. 700–708.

32. M. Komljenović, Z. Baščarević, N. Marjanović, and V. Nikolić, “External sulfate attack on alkali-activated slag”, *Construction and Building Materials*, Vol. 49, 2013, pp. 31–39.

33. A. Mobili, A. Belli, C. Giosuè, T. Bellezze, and F. Tittarelli, “Metakaolin and fly ash alkali-activated mortars compared with cementitious mortars at the same strength class”, *Cement and Concrete Research*, Vol. 88, 2016, pp. 198–210.

34. T. Bakharev, J.G. Sanjayan, and Y.-B. Cheng, “Resistance of alkali-activated slag concrete to acid attack”, *Cement and Concrete Research*, Vol. 33, No. 10, 2003, pp. 1607–1611.

35. T. Bakharev, “Resistance of geopolymer materials to acid attack”, *Cement and Concrete Research*, Vol. 35, No. 4, 2005, pp. 658–670.

36. O. Burciaga-Díaz, and J.I. Escalante-García, “Strength and Durability in Acid Media of Alkali Silicate-Activated Metakaolin Geopolymers”, *Journal of the American Ceramic Society*, Vol. 95, No. 7, 2012, pp. 2307–2313.

37. S.A. Bernal, E.D. Rodríguez, R. Mejía de Gutiérrez, and J.L. Provis, “Performance of alkali-activated slag mortars exposed to acids”, *Journal of Sustainable Cement-Based Materials*, Vol. 1, No. 3, 2012, pp. 138–151.

38. X.X. Gao, P. Michaud, E. Joussein, S. Rossignol, “Behavior of metakaolin-based potassium geopolymers in acidic solutions”, *Journal of Non-Crystalline Solids*, Vol. 380, 2013, pp. 95–102.

39. K. Bouguermouh, N. Bouzidi, L. Mahtout, L. Pérez-Villarejo, and M.L. Martínez-Cartas, “Effect of acid attack on microstructure and composition of metakaolin-based geopolymers: The role of alkaline activator”, *Journal of Non-Crystalline Solids*, Vol. 463, 2017, pp. 128–137.

40. RILEM TC 224-AAM. Alkali-Activated Materials: State-of-the-Art Report, RILEM State-of-the-Art Reports Volume 13, Eds. J.L. Provis and J.S.J. van Deventer, 2014, Springer/RILEM, Dordrecht, 396 pp.

41. J.S.J. van Deventer, J.L. Provis, P. Duxson, and D.G. Brice, “Chemical Research and Climate Change as Drivers in the Commercial Adoption of Alkali Activated Materials”, *Waste and Biomass Valorization*, Vol. 1, No. 1, 2010, pp 145–155.

42. British Standards Institution, “PAS 8820:2016 – Construction Materials – Alkali-activated cementitious material and concrete – Specification, *BSI*, London, UK, 2016.

43. M. Granizo, M. Blanco-Varela, and A. Palomo, “Influence of the starting kaolin on alkali-activated materials based on metakaolin. Study of the reaction parameters by isothermal conduction calorimetry”, *Journal of Materials Science*, Vol. 35, 2000, pp. 6309–6315.

44. Z. Zhang, H. Wang, J.L. Provis, F. Bullen, A. Reid, and Y. Zhu, “Quantitative kinetic and structural analysis of geopolymers. Part 1. The activation of metakaolin with sodium hydroxide”, *Thermochimica Acta*, Vol. 539, 2012, pp. 23–33.

45. H. Xu, and J.S.J. van Deventer, “The geopolymerisation of alumino-silicate minerals”, *International Journal of Mineral Processing*, Vol. 59, No. 3, 2000, pp. 247–266.

46. A. Buchwald, M. Hohmann, K. Posern, and E. Brendler, “The suitability of thermally

activated illite/smectite clay as raw material for geopolymer binders", *Applied Clay Science*, Vol. 46, No. 3, 2009, pp. 300–304.

47. H. Xu and J.S.J. Van Deventer, "Microstructural characterisation of geopolymers synthesised from kaolinite/stilbite mixtures using XRD, MAS-NMR, SEM/EDX, TEM/EDX, and HREM", *Cement and Concrete Research*, Vol. 32, No. 11, 2002, pp. 1705–1716.

48. M. Soutsos, A.P. Boyle, R. Vinai, A. Hadjierakleous, and S.J. Barnett, "Factors influencing the compressive strength of fly ash based geopolymers", *Construction and Building Materials*, Vol. 110, 2016, pp. 355–368.

49. H.K. Tchakoute, A. Elimbi, E. Yanne, and C.N. Djangang, "Utilization of volcanic ashes for the production of geopolymers cured at ambient temperature", *Cement and Concrete Composites*, Vol. 38, 2013, pp. 75–81.

50. R. Rajamma, J.A. Labrincha, and V.M. Ferreira, "Alkali activation of biomass fly ash–metakaolin blends", *Fuel*, Vol. 98, 2012, pp. 265–271.

51. A. Heath, K. Paine, S. Goodhew, M. Ramage, and M. Lawrence, "The potential for using geopolymer concrete in the UK", *Proceedings of the Institution of Civil Engineers - Construction Materials*, Vol. 166, No. 4, 2013, pp. 195–203.

52. Department for Energy and Climate Change, "Updated energy and emissions projections 2016", *DECC*, London, UK, March 2017.

53. A. Heath, K. Paine, M. McManus, "Minimising the global warming potential of clay based geopolymers", *Journal of Cleaner Production*, Vol. 78, 2014, pp. 75–83.

54. G.M. Reeves, I. Sims, and J.C. Cripps, "Clay Materials Used in Construction", Engineering Geology Special Publication, 21, *The Geological Society*, London, UK, 2006, 525 pp.

55. S. Seraj, R. Cano, R.P. Ferron, and M.C. Juenger "Calcined Shale as Low Cost Supplementary Cementitious Material", *Proceedings of the 1st International Conference on Calcined Clays for Sustainable Concrete*, RILEM Bookseries, Vol 10. Springer, Dordrecht, 2015, pp 531–537, Eds. K. Scrivener, A. Favier.

56. R. Arellano-Aguilar, O. Burciaga-Díaz, A. Gorokhovsky, and J.I. Escalante-García, "Geopolymer mortars based on a low grade metakaolin: Effects of the chemical composition, temperature and aggregate:binder ratio", *Construction and Building Materials*, Vol. 50, 2014, pp. 642–648.

57. A. Autef, E. Joussein, A. Poulesquen, G. Gasgnier, S. Pronier, I. Sobrados, J. Sanz, and S. Rossignol, "Influence of metakaolin purities on potassium geopolymer formulation: The existence of several networks", *Journal of Colloid and Interface Science*, Vol. 408, 2013, pp. 43–53.

58. M.A. Longhi, E.D. Rodríguez, S.A. Bernal, J.L. Provis, and A.P. Kirchheim, "Valorisation of a kaolin mining waste for the production of geopolymers", *Journal of Cleaner Production*, Vol. 115, 2016, pp. 265–272.

59. J.A. McIntosh, J. Kwasny, and M.N. Soutsos, "Evaluation of Northern Irish Laterites as Precursor Materials for Geopolymer Binders", *34th Cement and Concrete Science Conference*, Sheffield, UK, 14–17 Sep 2014, 6 p.

60. A. Mcintosh, S.E.M. Lawther, J. Kwasny, M.N. Soutsos, D. Cleland, and S. Nanukuttan, "Selection and characterisation of geological materials for use as geopolymer precursors", *Advances in Applied Ceramics*, DOI: 10.1179/1743676115Y.0000000055.

61. J. Kwasny, M.N. Soutsos, J.A. McIntosh, and D.J. Cleland, "banahCEM – comparison of properties of a laterite-based geopolymer with conventional concrete", *9th International Concrete Conference 2016. Environment, Efficiency and Economic Challenges for Concrete*, University of Dundee, Scotland, UK, 4–6 Jul 2016, pp. 383–394. Eds. M.R. Jones, M.D. Newlands, J.E. Halliday, L.J. Csetenyi, L. Zheng, M.J. McCarthy and T.D. Dyer.

62. V.A. Eyles, "Note on the Interbasaltic Horizon in Northern Ireland", *Quarterly Journal of the Geological Society*, Vol. 106, 1950, pp. 136–137.

63. M.R. Cooper, "Paleogene Extrusive Igneous Rocks", in "The Geology of Northern Ireland", (ed. W. I. Mitchell), Belfast, N. Ireland, *GSNI*, 2004, pp. 167–178.

64. http://www.banahuk.co.uk/

65. British Standards Institution, "BS EN 197-1:2011 – Cement. Composition, specifications and conformity criteria for common cements", *BSI*, London, UK, 2011.

66. British Standards Institution, "BS 812-2:1995 – Testing aggregates. Methods for determination of density", *BSI*, London, UK, 1995.

67. British Standards Institution, "BS 812-103.1:1985 – Testing aggregates. Method for determination of particle size distribution. Sieve tests," *BSI*, London, UK, 1985.

68. P.C. Aitcin, "High Strength Concrete (Modern Concrete Technology)", *E & FN Spon*, London, UK, 1998, 624 pp.

69. ASTM International, "ASTM C1012/C1012M-04 – Standard Test Method for Length Change of Hydraulic-Cement Mortars Exposed to a Sulfate Solution", Annual Book of ASTM Standards, ASTM International, West Conshohocken, United States, 2004.

70. ASTM International, "ASTM C267-01 – Standard Test Methods for Chemical Resistance of Mortars, Grouts, and Monolithic Surfacings and Polymer Concretes", Annual Book of ASTM Standards, ASTM International, West Conshohocken, United States, 2001.

71. S. Diamond, "Mercury porosimetry: An inappropriate method for the measurement of pore size distributions in cement-based materials", *Cement and Concrete Research*, Vol. 30, No. 10, 2000, pp. 1517–1525.

72. K. Okada, A. Ooyama, T. Isobe, Y. Kameshima, A. Nakajima, and K.J.D. MacKenzie, "Water retention properties of porous geopolymers for use in cooling applications", *Journal of the European Ceramic Society*, Vol. 29, No. 10, 2009, pp. 1917–1923.

73. Z. Zhang, Xiao Yao, and Huajun Zhu, "Potential application of geopolymers as protection coatings for marine concrete: II. Microstructure and anticorrosion mechanism", *Applied Clay Science*, Vol. 49, No. 1-2, 2010, pp. 7–12.

74. D. Winslow, and D. Liu, "The pore structure of paste in concrete", *Cement and Concrete Research*, Vol. 20, No. 2, 1990, pp. 227–235.

75. C.S. Poon, and Y.L. Wong, L. Lam, "The influence of different curing conditions on the pore structure and related properties of fly-ash cement pastes and mortars", *Construction and Building Materials*, Vol. 11, No. 7-8, 1997, pp. 383–393.

76. M. Sahmaran, O. Kasap, K. Duru, and I.O. Yaman, "Effects of mix composition and water–cement ratio on the sulfate resistance of blended cements", *Cement and Concrete Composites*, Vol. 29, No. 3, 2007, pp. 159–167.

77. X. Gao, B. Ma, Y. Yang, and A. Su, "Sulfate Attack of Cement-Based Material with Limestone Filler Exposed to Different Environments", *Journal of Materials Engineering and*

Performance, Vol. 17, No. 4, 2008, pp. 543–549.

78. O.S.B. Al-Amoudi, "Attack on plain and blended cements exposed to aggressive sulfate environments", *Cement and Concrete Composites*, Vol. 24, No. 3–4, 2002, pp. 305–316.

79. T. Aye, and C.T. Oguchi, "Resistance of plain and blended cement mortars exposed to severe sulfate attacks", *Construction and Building Materials*, Vol. 25, No. 6, 2011, pp. 2988–2996.

80. M. Santhanam, M.D. Cohen, J. Olek, "Mechanism of sulfate attack: A fresh look: Part 1: Summary of experimental results", Cement and Concrete Research, Vol. 32, No. 6, 2002, pp. 915–921.

81. D. Bonen, and M.D. Cohen, "Magnesium sulfate attack on portland cement paste-I. Microstructural analysis", *Cement and Concrete Research*, Vol. 22, No. 1, 1992, pp. 169–180.

82. S.N. Ghosh, "IR spectroscopy", In: "Handbook of Analytical Techniques in Concrete Science and Technology. Principles, Techniques, and Applications", Eds. V.S. Ramachandran and J.J. Beaudoin, *Noyes Publications/William Andrew Publishing*, Park Ridge, New Jersey, USA/Norwich, New York, USA, 1999, pp. 174–204.

83. A. Peyvandi, D. Holmes, P. Soroushian, and A.M. Balachandra, "Monitoring of Sulfate Attack in Concrete by ^{27}Al and ^{29}Si MAS NMR Spectroscopy", *ASCE Journal of Materials in Civil Engineering*, Vol. 27, No. 8, 2015, 10 pp.

84. A. Putnis, B. Winkler and L. Fernandez-Diaz, "In Situ IR Spectroscopic and Thermogravimetric Study of the Dehydration of Gypsum", *Mineralogical Magazine*, Vol. 54, No. 374, 1990, pp. 123–128.

85. M.A.M. Ariffin, M.A.R. Bhutta, M.W. Hussin, M. Mohd Tahir, and N. Aziah, "Sulfuric acid resistance of blended ash geopolymer concrete", *Construction and Building Materials*, Vol. 43, 2013, pp. 80–86.

86. R.L Frost, J.T. Kloprogge, "Infrared emission spectroscopic study of brucite", Spectrochimica Acta Part A: Molecular and Biomolecular Spectroscopy, Vol. 55, No. 11, 1999, pp. 2195–2205.

87. V. Pavlík, "Corrosion of hardened cement paste by acetic and nitric acids part II: formation and chemical composition of the corrosion products layer", *Cement and Concrete Research*, Vol. 24, No. 8, 1994, pp. 1495–1508.

88. T. Gutberlet, H. Hilbig, and R.E. Beddoe, "Acid attack on hydrated cement — Effect of mineral acids on the degradation process", *Cement and Concrete Research*, Vol. 74, 2015, pp. 35–43.

89. J.C. Doadrio, D. Arcos, M.V. Cabañas, and M. Vallet-Regí, "Calcium sulphate-based cements containing cephalexin", Biomaterials, Vol. 25, No. 13, 2004, pp. 2629-2635.

90. A. Putnis, B. Winkler and L. Fernandez-Diaz, "In Situ IR Spectroscopic and Thermogravimetric Study of the Dehydration of Gypsum", *Mineralogical Magazine*, Vol. 54, No. 374, 1990, pp. 123–128.

91. M.A.M. Ariffin, M.A.R. Bhutta, M.W. Hussin, M. Mohd Tahir, and N. Aziah, "Sulfuric acid resistance of blended ash geopolymer concrete", *Construction and Building Materials*, Vol. 43, 2013, pp. 80–86.